

**To Investigate Flexural and Compressive Strength of High  
Strength Concrete by Addition of Basalt and Steel Fibers at  
Elevated Temperature**

**A Thesis of Master of Science**

**Submitted By**



**Mushtaq Ahmad**

**(NUST-2019-00000318660-MCE)**

**Master of Science in Structural  
Engineering**

**Military College of Engineering**

**National University of Sciences and Technology (NUST)  
Islamabad, Pakistan (2023).**

**To Investigate Flexural and Compressive Strength of High Strength Concrete by Addition of Basalt and Steel Fibers at Elevated Temperature.**

Author

**MUSHTAQ AHMAD**

Reg Number

**(NUST-2019-00000318660-MCE)**

A thesis submitted in partial fulfillment of the requirements for  
the degree of

**MS STRUCTURAL ENGINEERING**

Thesis Supervisor:

DR. M Naveed Aslam Metla

Thesis Supervisor's Signature:



---

DEPARTMENT OF STRUCTURAL ENGINEERING  
MILITARY COLLEGE OF ENGINEERING, RISALPUR  
NUST, PAKISTAN

## Thesis Acceptance Certificate

It is certified that the final copy of the MS thesis written by Accredited that the final copy of **MR. MUSHTAQ AHMAD**. Reg. No. **00000318660** of **Military College of Engineering, National University of Sciences & Technology, Risalpur Campus** has been assessed, discovered complete in all respects as per NUST Legislation / Regulations, is free of copyright infringement, errors, and mistakes, and is recognized as partial fulfilment for award of **MS degree in Structural Engineering**. It is also confirmed that any necessary adjustments indicated by the GEC members of the academic have been incorporated into the thesis.

Supervisor: \_\_\_\_\_



LI Col  
GSO-1 (Civ Engg Wing)  
(Mil College of Engineering)

Assistance professor **Dr. M Naveed Aslam Metla**  
Department of Structural Engineering

## Declaration

I certify that this research work titled “*To Investigate Flexural and Compressive Strength of High Strength Concrete by Addition of Basalt and Steel Fibers at Elevated Temperature*” is my work. The work has not been presented elsewhere for assessment. The material that has been used from other sources has been properly acknowledged/ referred to.



Signature of Student

MUSHTAQ AHMAD

NUST-2019-00000318660-MCE

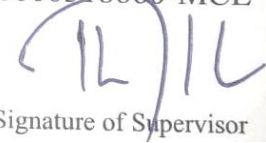
## Plagiarism Certificate (Turnitin Report)

This thesis has been checked for Plagiarism. Turnitin report endorsed by Supervisor is attached.



Signature of Student  
MUSHTAQ AHMAD  
Registration Number

NUST-2019-00000318660-MCE



Signature of Supervisor

## **Copyright Statement**

- Copyright in text of this thesis rests with the student author. Copies (by any process) either in full or in extracts, may be made only in accordance with instructions given by the author and lodged in the Library of Military College of Engineering, Risalpur. Details may be obtained by the Librarian. This page must form part of any such copies made. Further copies (by any process) may not be made without the permission (in writing) of the author.
- The ownership of any intellectual property rights which may be described in this thesis is vested in Military College of Engineering, Risalpur, subject to any prior agreement to the contrary, and may not be made available for use by third parties without the written permission of the MCE, which will prescribe the terms and conditions of any such agreement.
- Further information on the conditions under which disclosures and exploitation may take place is available from the Library of Military College of Engineering, Risalpur.

## **Acknowledgement**

I find no appropriate words to express and elaborate my deepest sense of gratitude to Almighty ALLAH, Mercy, Kindness, and Courtesy was but: everything for me, who brought me into being and have quested me with enlightenment, wisdom, and power to explore. First and foremost, I express my profound gratitude to my parents and to my siblings for providing me with unfailing support and continuous encouragement throughout my years of study and through the process of research and writing this thesis. This accomplishment would not have been possible without them.

I would want to express my gratitude to Dr Muhammad Rizwan my advisor Dr M Naveed Aslam Metla and co-supervisor Dr Muhammad Faisal Javed. Their unending motivation, and guidance enabled me to accomplish my research project. Furthermore, I want to express my thanks to the Military College of Engineering's academic staff, who provided a lot of knowledge during academic session in the postgraduate program.

There are several people without whom support this thesis might not have been written, and to whom I am gratefully indebted. I owe my sincere gratitude to the faculty of MCE, who were more than generous with their expertise and precious time. I am grateful to all my colleagues in class 2019 (SE-06), especially to Engr Burhan Ullah, Engr Kashan Nisar, Engr Ahmad Roydad, Engr Noman Qamar and Engr Ahsan Mehmood for their sincere help and guidance during this thesis work. I am also thankful to the laboratory staff of structure dynamics and the concrete lab of MCE.

## **Dedication**

This thesis is dedicated to **Hazrat Muhammad (SAW)** minaret of knowledge and wisdom, my beloved **parents** and my beloved **siblings** who always supported me through thick and thin of my life, my **friends** who cheered me when I was sad and always motivated me.

## Abstract

High-strength concrete is characterized by dense microstructure, lower porosity, and high durability. Still, it exhibits poor mechanical performance when subjected to elevated temperatures because of its inability to facilitate adequate water vapor dissipation, leading to cracking and spalling. Hybrid fibers were integrated into the HSC matrix to address this inherent limitation. A hybrid fiber-reinforced concrete (HFRC) comprises two or more types of fibers blended within the concrete mixture. HFRC has top-notch thermo-mechanical properties. This research aims to enhance the mechanical properties and thermal stability of HSC under thermal stress conditions. A systematic investigation assessed the mechanical properties, mass degradation, and surface cracking exposed to elevated temperatures. In this study, hybrid fibers (HF) were added to HSC specimens with varying proportions of 0.25%, 0.5%, 0.75%, and 1%, and then exposed to temperatures of 300°C, 600°C, and 800°C at a rate of 5°C/min. Empirical findings revealed that hybrid fiber-reinforced concrete exhibited superior mechanical properties relative to the control specimen. This improvement can be due to the basalt fibers filler properties and the hybrid fiber ability to bridge cracks. 0.5% hybrid fiber reinforced concrete demonstrated optimal mechanical properties, whereas concrete with 0.75% hybrid fiber exhibited the least mass degradation. The toughness was increased with the increasing content of HF in concrete. It was noted that too many hybrid fibers in concrete can have adverse effects, resulting in clumping. This is not only causing voids but also diminishes the amount of cement present, which in turn minimizes the strength of the concrete.

**Key words:** High Strength Concrete (HSC), Hybrid Fiber Reinforced High Strength Concrete (HFR-HSC), Hybrid Fiber Reinforced Concrete (HFRC), Basalt fiber (BF), Steel fiber (SF), Compressive and Flexural Strength.

# Table of Contents

Thesis Acceptance Certificate .....	iii
Declaration .....	iv
Plagiarism Certificate (Turnitin Report) .....	v
Copyright Statement.....	vi
Acknowledgement.....	vii
Dedication .....	viii
Abstract .....	ix
List of Tables.....	xiii
List of Figures .....	xiv
List of Abbreviations.....	xv
CHAPTER 1.....	1
INTRODUCTION.....	1
1.1 General .....	1
1.2 Objectives.....	3
1.3 Research Overview .....	3
1.4 Research Significance .....	4
1.5 Thesis Overview.....	4
CHAPTER 2 .....	6
LITERATURE REVIEW .....	6
2.1 General .....	6
2.2 Basalt Fiber .....	6
2.2.1 Properties of Basalt Fiber.....	7
2.3 Steel Fiber .....	9
2.3.1 Application of Steel Fibers .....	10
2.4 High Strength Concrete .....	11
2.5 Silica Fume.....	12
2.5.1 Uses of Silica Fume .....	12
2.5.2 Chemical Reaction of Silica Fume` .....	13
2.6 Testing Procedure Based on Loading and Heating Regime.....	13
2.7 Previous Research on the Mechanical Properties of Concrete at High Temperatures.....	14
2.7.1 Compressive Strength .....	14

2.7.2	Flexural Strength Test.....	16
2.7.3	Elastic Modulus .....	18
2.7.4	Stress-Strain Compressive Curve .....	19
CHAPTER 3 .....		21
EXPERIMENTAL PROGRAM .....		21
3.1	General .....	21
3.2	Formulation of Experiments for Material Properties .....	21
3.3	Materials.....	22
3.3.1	Cement .....	22
3.3.2	Fine Aggregates .....	22
3.3.3	Coarse Aggregates .....	23
3.4	Admixture.....	25
3.4.1	Super Plasticizer.....	25
3.4.2	Silica Fume .....	25
3.5	Fiber Additives .....	26
3.5.1	Importance of Fibers .....	26
3.5.2	Steel Fiber .....	26
3.5.3	Basalt Fiber .....	26
3.6	Mix Proportions.....	26
3.7	Sample Preparation .....	27
3.8	Material Property Tests .....	29
3.9	Fire Loading Characteristics .....	29
3.10	Target Temperature, Heating Rate, and Hold Time for Test Method.....	29
3.11	Test Apparatus and Procedure.....	30
3.11.1	Compressive Strength Test .....	33
3.11.2	Flexural Strength Test.....	33
3.11.3	Stress-Strain Curve .....	34
3.11.4	Modulus of Elasticity (E).....	34
3.11.5	Mass Loss.....	34
CHAPTER 4 .....		35

RESULTS AND DISCUSSIONS .....	35
4.1    General .....	35
4.2    Elevated Temperature Mechanical Properties.....	35
4.2.1    Compressive Strength .....	35
4.2.2    Stress-Strain Curve .....	37
4.2.3    Modulus of Elasticity E .....	41
4.2.4    Compressive Failure Mode .....	42
4.2.5    Load Vs Displacement Variations .....	44
4.2.6    Flexural Strength.....	45
4.2.7    Energy Absorption Capacity (Toughness).....	47
4.2.8    Compressive Toughness Index .....	48
4.2.9    Crack Energy and Toughness Index .....	49
4.2.10    Mass Loss.....	51
4.2.11    Visual Inspection .....	52
CHAPTER 5 .....	56
CONCLUSION AND RECOMMENDATION.....	56
5.1    Conclusion.....	56
5.2    Recommendations .....	57
REFERENCES .....	59

## **List of Tables**

Table 1: Properties of Basalt Fibers. ....	8
Table 2: Chemical Composition of Basalt Fiber. ....	9
Table 3: Properties of Steel Fibers. ....	11
Table 4: Raw Ingredients of Cement. ....	22
Table 5: Properties of Aggregates. ....	22
Table 6: Gradation of Fine Aggregate. ....	23
Table 7: Gradation of Coarse Aggregate. ....	24
Table 8: Chemical Properties of Superplasticizer. ....	25
Table 9: Properties of Silica Fume. ....	25
Table 10: Mix Design in Kg/m <sup>3</sup> . ....	27
Table 11: Overview of Cylinders and Beams Samples with Temperatures. ....	28

## List of Figures

Figure 1: Chopped Basalt Fibers.....	8
Figure 2: Steel Fibers.....	11
Figure 3: Silica Fume.....	12
Figure 4: Gradation Curve of Fine Aggregate and ASTM Lower and Upper Limits.....	23
Figure 5: Sieve Shaker.....	24
Figure 6: K-Type Thermocouples Drilled Inside the Specimen.....	30
Figure 7: Temperature Vs Time Graph of Prism Beams.....	32
Figure 8: Electric Furnace for Heating the Samples to Targeted Temperatures.....	32
Figure 9: Compression Testing Machine.....	33
Figure 10: Flexural Test Assembly ASTM C (293/293-16).....	33
Figure 11: Universal Hydraulic Testing Machine for Flexural Strength Test.....	34
Figure 12: Variation of Compressive Strength as A Function of Temperature.....	37
Figure 13: Fiber Crack Arresting Mechanism.....	39
Figure 14: Stress-Strain Curve of Cylinders.....	40
Figure 15: Modulus of Elasticity Of Concrete Cylinders.....	42
Figure 16: Compressive Failure Mode of Cylinders at Targeted Temperatures.....	44
Figure 17: Load Vs Deflection Curve of Beams with Different Elevated Temperatures. .....	45
Figure 18: Flexural Strength of Beams with Different Temperatures.....	46
Figure 19: Compressive Toughness of Concrete Cylinders at Different Temperatures.....	48
Figure 20: Compressive Toughness Index is a Function of Temperature.....	49
Figure 21: Crack Energy is a Function of Temperature.....	49
Figure 22: Flexural Toughness Index is a Function Of Temperature.....	50
Figure 23: Mass Loss of Concrete Cylinders with Varying Temperature, (b) Mass Loss of Concrete Beams with Varying Temperature.....	51
Figure 24: External Surface of Concrete Cylinders at Different Temperature.....	54
Figure 25: External Surface of Concrete Beams at Different Temperature.....	55

## **List of Abbreviations**

HSC	High strength Concrete
HFRC	Hybrid Fiber Reinforced Concrete
HFR-HSC	Hybrid Fiber Reinforced High Strength Concrete
FRC	Fiber Reinforced Concrete
HF	Hybrid Fiber
SF	Steel Fiber
BF	Basalt Fiber
CS	Control Sample
ASTM	American Society for Testing Material
CH	Calcium Hydroxide
CSH	Calcium Silicate hydrate
TI	Toughness Index
MT	Mass at Target Temperature
ACI	American Concrete Institute

# CHAPTER 1

## INTRODUCTION

### 1.1 General

Concrete is prevalent in construction and is often employed in building projects. Over their functional lifetime, civil engineering structures face environmental risks, including earthquake forces and fire hazards[1–3]. Fire exposure can damage concrete structures by reducing their strength and possibly leading to sudden breaks, even though concrete tends to be more resistant to fire than metal, as a six-story building 'Industry Facilitation Centre in Islamabad, Pakistan, experienced extensive concrete chipping and notable warping of its reinforcement and its members, after being exposed to fire [4], [5]. Hence, it is crucial to comprehend how fire affects concrete's material and chemical characteristics to make structures capable of enduring high temperatures during fire exposure.

Increased interest in high-strength concrete (HSC) can be attributed to its superior compressive strength, which reduces the weight and size of structural elements, along with its refined microstructure, lower porosity, and enhanced durability[6–8]. When HSC is subjected to elevated temperature, may cause thermal cracking and unfavorable chemical changes, compromising its structural application. The accumulation of substantial pore pressure inside the HSC may be a potential factor contributing to explosive spalling [9]. The evaporation of free and chemically bound water produced vapor pressure, resulting in tensile stress within the concrete. This can lead to concrete spalling[10–12]. The thermal gradient may also contribute to spalling the concrete's exterior surface from the interior layer [13], [14], Therefore, it is significant to investigate the mechanical behavior of fiber-reinforced concrete (FRC) at high temperatures to overcome the fire risk. FRC has top-notch thermo-mechanical properties over conventional concrete and gained increasing interest in the recent few years [15]. such as high compressive, flexural, and tensile strength [16–20], good impact resistance and ductility [21], [22], better energy absorption capability, reduce internal pore pressure in concrete [7]. Previous literature shows that numerous investigations were carried out on FRC with different fibers like basalt, steel, polypropylene, glass, and banana threads [23], and studied their mechanical properties at elevated temperatures. Steel fiber reinforced concrete (SFRC) shows superior residual mechanical properties when subjected to higher temperatures than plain concrete. It can provide more effective

resistance against explosive spalling [24], [25]. incorporation of basalt fibers into concrete reduced vapor pressure and improved residual mechanical properties [12]. Thus, integrating steel and synthetic mineral fibers to make hybrid fiber-reinforced concrete thermally stable enhances mechanical properties and resistance against fire.

In this topic hybrid fiber reinforced high strength concrete (HFR-HSC) prepared by mixing steel and basalt fiber under elevated temperature is investigated. Currently, the construction industry offers a diverse range of organic and inorganic fibers. However, a significant number of these fibers exhibit deficiencies in terms of durability, structural strength, or affordability for use in moderate loadings. Currently, the building sector is seeing a high demand for BF. Basalt fiber is derived from a natural volcanic basalt rock, which serves as the primary raw material. The process of producing basalt fiber involves subjecting the raw material to high temperatures within a furnace, namely in the range of 1450 to 1500<sup>0</sup>c, resulting in its melting. Subsequently, the liquefied substance is compelled to pass through a crucible bushing composed of platinum and rhodium, resulting in the formation of fibers [26]. In general, basalt fibres exhibit several advantageous characteristics that position them as a workable replacement for glass fibres in the reinforcement of composites utilised across various industries including marine, motor vehicles athletic devices, civil engineering. The initial expense associated with basalt fibers is contingent upon the quality and composition of chemicals of the source substance, resulting in production of several types of fibers with distinct thermal, chemical, and mechanical properties [26].

The utilization of hybrid fiber-reinforced concrete (HFRC) in the construction sector has experienced significant advancements in recent decades. Moreover, HF has different lengths, forms, modulus of elasticity, and density that can improve overall mechanical properties and resistance to cracks at different levels in the concrete matrix when subjected to mechanical stress [27–29]. Adding steel and basalt fibers to concrete is more fire-resistant and shows better residual mechanical capability when subjected to elevated temperatures than plain concrete. Steel fibers play a crucial role in HFRC by offering bridging capabilities to improve strength, toughness, and strength retention at higher temperatures than conventional concrete [30]. Based on the findings, it was seen that a high steel-fiber dosage decreases compressive strength. This was attributed to the higher density of steel fibers, which resulted in local gaps within the concrete [31]. Basalt fibers also improve stability by the filler effect to strengthen concrete and restrict

crack propagation by bridging development. As temperature increases, partially melted basalt fibers provide channels for water vapor to evaporate, thus decreasing pore pressure so less strength reduction occurred compared to the control sample. Any increase beyond the optimum percentage strength is reduced. This strength reduction could be due to the clumping of the fibers, which forms more voids and creates weak zones within the concrete [32]. Thus, adding basalt and steel fibers in HSC can be reliable and improve strength at elevated temperatures.

This research investigates hybrid fiber-reinforced high-strength concrete's residual compressive and flexural strength, modulus of elasticity, toughness, visual inspection, and mass loss at elevated temperatures. Hybrid fibers (HF), with various types, tensile strength, modulus of elasticity, length, and morphologies, can improve concrete mechanical properties and fracture resistance at different stages. In addition, basalt fibers (BFs) resist cracks at the micro and macro levels, while steel fibers (SFs) resist at the macro level. Basalt fibers fill the remaining voids, and the high modulus of elasticity of HF makes concrete denser; further, the crystallization process starts on the surface of BF, making concrete stable at a high temperature. Therefore, varying percentages of HF are induced in concrete and study residual strength. In this formulation, different concentrations of HF, i.e., 0.25%, 0.5%, 0.75%, and 1%, were added by volume of concrete. As the authors know, no study has been conducted on these specific percentages of hybrid fibers in HSC. The lengths of steel and basalt were 24mm and 18mm.

## **1.2 Objectives**

- To study compressive and flexural strength of hybrid fiber reinforced high strength concrete (steel and basalt fibers).
- To determine the efficient ratio of basalt-steel fiber for compressive, flexural, elastic modulus and toughness of hybrid fiber-reinforced concrete.

## **1.3 Research Overview**

The following tasks are carried out to achieve research objectives.

- Literature review.
- Test set up compression test, Flexural test assembly and steel assembly for furnace.

- Execute tests at elevated temperature.
- Evaluate the experimental results.
- Conclusion and recommendations.

#### **1.4 Research Significance**

In high rise buildings, nuclear sector and offshore structure uses of high strength concrete has been increasing for last two decade. HSC have more advantages over normal strength concrete its b/c of compact microstructure, high durability, low permeability, high compressive strength, lower porosity and decreasing cross section of structural member. Furthermore, the exponential growth in the application of concrete as a building material has demonstrated that the financial investment needed to sustain the intended durability of concrete during its lifespan is not cost-effective. It is feasible to make concrete having high compressive strength. At elevated temperature HSC behave differently and collapse as compared to Normal strength concrete (NSC). HSC perform poorly when expose to high temperature and thermal cracks are generated. HSC has less inter. The HSC has less interconnected smaller pores and high density which prevent rapid escape of water vapor under elevated temperature exposure. Then concrete get failed in an explosive manner when vapor pressure surpasses tensile strength. To overcome this issue and improving residual strength fiber reinforced concrete is excellent substitute.

FRC has high tensile and compressive strength as compared to conventional concrete, excellent energy absorption capacity, impact resistance, reduce crack propagation, resistance to freezing and thawing, thermal stability, reducing spalling of concrete. This research investigates residual compressive and flexural strength of hybrid fiber reinforced high strength concrete at elevated temperature. Hybrid fibers, with a variety of type, tensile strength, modulus of elasticity, length, and morphologies, have the potential to enhance the mechanical properties and fracture resistance of cement-based composites at various phases. Therefore, varying proportions of hybrid fiber is induced in concrete and then study the residual strength.

#### **1.5 Thesis Overview**

**Chapter 1** introduction of HSC and its behavior when exposed to elevated temperatures, research objectives and research significance has been discussed.

**Chapter 2** A brief literature review about properties of SFs and BFs in general and their need to use in high strength concrete. Performance of HSC has been discussed in detail at elevated temperature in addition to that test methods (residual) have been discussed.

**Chapter 3** This chapter discuss test setup and equipment's used to valuate mechanical properties. Moreover, it describes an overview of the tests and methods to find out mechanical properties.

**Chapter 4** This chapter is concern with analyze, evaluate, and discuss the results of material property tests. Results of thermal and mechanical properties of specimens.

**Chapter 5** Brief description about conclusions and recommendations

## **CHAPTER 2**

### **LITERATURE REVIEW**

#### **2.1 General**

In this chapter briefly discusses basalt and steel fiber, their production and usage in concrete. Steel and basalt fibers' properties at normal temperature have been explored, and literature on HSC properties at elevated temperature has been discussed. In the construction industry, concrete is mostly used due to its high elastic modulus, compressive strength, molded to any shape, simplicity of preparation, water tightness, resistance to corrosive agents and increased fire resistance. In high building and offshore structures HSC is preferred on NSC it's b/c of high compressive strength, durability, and compact microstructure. Since concrete was initially introduced to the construction industry, the quality of the material has steadily improved. The compressive strength of concrete is a direct predictor of its durability; concrete with a higher compressive strength has a bigger modulus of elasticity, tensile strength, and lower permeability, and so is more durable. The usage of HSC has become quite prevalent since the development of superplasticizers (SP) or high-range water reducers (HRWRs). In terms of greater durability and economics, HSC has a lot of benefits. Because of the smaller cross sections, the use of HSC in high-rise building columns has become a supplementary technique in contemporary construction practices. Numerous investigations have been undertaken to examine the performance of concrete at escalating temperatures. When compared to NSC, the data demonstrate that HSC performs poorly at higher temperatures, despite its superior performance in all other situations.

#### **2.2 Basalt Fiber**

The construction industry currently offers a wide range of organic and inorganic fibers. However, a significant portion of these fibers suffer from deficiencies in terms of durability, structural strength, or affordability when used under moderate loadings. Currently, the building sector is utilizing basalt fiber (BF) as a highly sought-after fiber. Basalt rocks undergo a process of melting at a temperature range of around 1500 to 1700 degrees Celsius. The substance undergoes rapid melting and afterward solidifies into a glassy, virtually amorphous state. The composition of several basaltic rocks is predominantly comprised of two crucial minerals, namely plagiocene and pyroxene, which collectively account for around 80% of their overall composition. Basalt is mainly

composed of silicon oxide. Silicon dioxide ( $\text{SiO}_2$ ), with an acceptable weight percentage range of 43.3-47%, is the predominant component, followed by aluminum oxide ( $\text{Al}_2\text{O}_3$ ) with an optimal range of 11-13% weight percentage. The composition of calcium oxide ( $\text{CaO}$ ) and magnesium oxide ( $\text{MgO}$ ) exhibits a significant degree of similarity, with the best range for  $\text{CaO}$  falling within 10-12% and the optimal range for  $\text{MgO}$  falling between 8-11%. The presence of other oxides is often observed at levels below 5%.

### **2.2.1 Properties of Basalt Fiber**

Basalt has a wide temperature range of applicability, spanning from extremely cold temperatures of about  $-200^\circ\text{C}$  to relatively high temperatures of  $700\text{--}800^\circ\text{C}$  [33]. It has a superior operational temperature range and enhanced tensile strength compared to E-glass fiber. Additionally, it demonstrates commendable resistance against chemical aggression, impact loads, and fire while emitting fewer toxic fumes [34]. The utilization of basalt fiber reinforcement presents a promising alternative approach within the fiber-reinforced polymer (FRP) strengthening systems. The study revealed that the tensile strength of basalt fiber was approximately 30% and 60% of the tensile strength exhibited by carbon fiber and high-strength glass (S-glass) fiber, sequentially. The decrease in strength was notably more pronounced in the carbon and glass fibers, but the basalt fibers exhibited a retention of around 90% of their strength at normal temperatures up to  $600^\circ\text{C}$  [35]. Compressive, flexural, and split tensile strength of BFRC improved by 0.18–4.68%, 14.08–24.34%, and 6.30–9.58% correspondingly. When the length of the BF rises to 22 mm, the related strengths experience an increase ranging from 0.55% to 5.72%, 14.96% to 25.51%, and 7.35% to 10.37%, respectively [36]. The heat resistance of basalt filament was examined by experimental means. The experimental findings indicate that the resistance remains consistent until reaching a temperature of  $350^\circ\text{C}$ , after which a little decline occurs till reaching  $500^\circ\text{C}$ . At a temperature of  $700^\circ\text{C}$ , a fracture of the basalt filament was seen, resulting in the breakage of nearly all the filaments at  $800^\circ\text{C}$  [37]. The tensile strength of these fibers is often somewhat higher than that of E-glass fibers and significantly more than that of SF. The observed increase in strength was more pronounced when utilizing longer, 50 mm BF compared to 36 mm BF [38]. Scanning electron microscopy (SEM) pictures reveal that a favorable adhesion between the surface of BF and the hydrated cement matrix is achieved during the initial stages of development. The optimal proportion of BF is around 0.3% of their volume [36]. Heat transfer is considerably reduced at all temperature levels when a significant

quantity of glass and basalt fiber is used [39]. Basalt fibers significantly improved the HPFRC's tensile splitting strength and flexural strength. The ITZ between the aggregates and the paste in HPFRC was investigated by the utilization of a field emission scanning electron microscope (FESEM). The examination demonstrated that integrating Basalt fibers resulted in an enhancement of the ITZ. The incorporation of BF at concentrations of 1%, 2%, and 3% resulted in an enhancement of the flexural strength of the concrete by 17.1%, 34.14%, and 26.14%, correspondingly, compared to the flexural strength of the control sample [40]. Nevertheless, producers of basalt provide basalt continuous strands and fabric that exhibit a comparative strength increase of around 30%, stiffness enhancement of 15-20%, and weight reduction of 8-10% when compared to E-glass materials [26]. The concrete's mass loss in the case of HFRC with a 12 mm basalt fiber was lower than that seen with 25, 37, and 50mm fibers. This may be attributed to the fact that using longer fibers with higher content resulted in the production of more porous concrete. Consequently, this porous concrete included more free water that evaporates at rising temperatures [41]. The most crucial constituent of basalt fiber is  $\text{SiO}_2$ ,  $\text{Al}_2\text{O}_3$ ,  $\text{Fe}_2\text{O}_3$  and  $\text{MgO}$ .



**Figure 1:** Chopped Basalt Fibers.

**Table 1:** Properties of Basalt Fibers.

Fiber length	18mm
Thickness	18micro meter
Modulus of elasticity	75GPA
Strength	1800Mpa
Elongation	2.6%

**Table 2:** Chemical Composition of Basalt Fiber.

SiO <sub>2</sub>	Al <sub>2</sub> O <sub>3</sub>	Fe <sub>2</sub> O <sub>3</sub>	MgO	CaO	Na <sub>2</sub> O	K <sub>2</sub> O	TiO <sub>2</sub>	P <sub>2</sub> O <sub>5</sub>	MnO	Cr <sub>2</sub> O <sub>3</sub>
52.5%	17.5%	10.3%	4.63%	8.59%	3.34%	1.46%	1.38%	0.28%	0.16%	0.06%

### 2.3 Steel Fiber

Resistance to fire of SFRC has garnered significant interest, and many studies focused on examining the residual qualities of SFRC. The use of SFRC demonstrates superior residual mechanical qualities in comparison to plain concrete when subjected to extreme temperatures. Additionally, SFRC indicates a higher level of effectiveness in mitigating the potential hazard of explosive spalling [42]. Incorporating polypropylene or steel fibers into conventional concrete can enhance strength and increase fire resistance properties. This delays the occurrence of cracks and the potentially hazardous phenomenon of explosive concrete spalling [43].

Combining hybrid fibers in ultra-high-performance concrete has a high initial crack and ultimate strength. The compressive strength, strength at an initial crack, and maximum tensile strength of UHPC with 1.5% steel fiber is 149Mpa, 9.8Mpa, and 14.3Mpa while UHPC containing SF 1.0%-Bf 0.5% have 128 Mpa, 13.42Mpa and 14.74Mpa [20]. The findings revealed that using 0.25% SF by volume enhances the compressive, tensile, and shear strength within a range of 8-26%, 7-197%, and 2-21% sequentially [44]. The incorporation of SF is beneficial in mitigating the propagation of crack width. A higher concentration of steel fibers showed a notable crack width reduction [45]. A combination of hybrid polypropylene (PP) and steel fibers effectively eliminated the occurrence of explosive spalling, even when a low dose of fibers was employed. This may be due to a notable enhancement in permeability. In the current investigation, the necessary PP fiber concentration to avoid spalling is 4 kg/m<sup>3</sup>. For specimens with Polypropylene-Steel fiber dosage (Pa-Sb; a=4, 6; b=79, 157, 236) kg/m<sup>3</sup>, the specimens stayed intact following heating, and explosive spalling was prevented [24]. The recycled aggregate, compressive strength decreases with rising temperatures. However, the inclusion of steel fibers effectively reduces this adverse effect. The steel-fiber RAC with silica fume has outstanding compressive performance in high-temperature environments because of the coupling effect of the two materials [46]. Steel fibers may increase a material's ability to withstand high temperatures, and the extent of the enhancement depends on the amount of fiber used. Steel fibers used to fiber-reinforced concrete increase its toughness

compared to concrete without steel fibers. The relative residual compressive strength of SFRC has a positive correlation with increasing fiber content at a temperature of 400 °C. Nevertheless, that is not always the case when the temperature hits 600 °C [47]. The sensitivity of the rate of SFRC is shown to grow as the volume fraction of fibers increases until it reaches a critical value of around 1.5% to 2.5%. However, beyond this critical value, the rate sensitivity diminishes when the dose of fibers exceeds 2.5% [48]. The specimens were directly exposed to the flame of fire and temperature were measured with an infrared thermometer. Once subjected to the fire test, it was seen that specimens containing a 1% addition exhibited superior performance compared to specimens containing a 2% addition. The strength of the modifier was shown to be better than without addition [43]. Most studies have shown that when the concentration of steel fiber reached 1%, the most effect was seen. The incorporation of SF in concrete demonstrated a notable enhancement in the flexural strength, particularly when the exposure temperature was below 800°C. The effectiveness of the steel fiber diminishes progressively due to oxidation and corrosion once the temperature exceeds 800°C. It was observed that the residual flexural strength of single steel FRC exhibited the greatest value [42]. In the experimental concrete, RC80/60 BN type SF were included at varying rates of 0%, 0.5%, 1%, and 1.5% by volume. In relation to the steel-fiber additive, the samples with a steel-fiber additive content of 1.0% exhibited the lowest decrease in strength at temperatures of 900°C, 1100°C, and 1200°C. However, for a temperature of 1000°C, the samples with an SF additive content of 1.5% showed the least strength loss. The effectiveness of steel-fiber additive was destroyed when exposed to temperatures over 1000<sup>0</sup>c [49]. SFRC subjected to elevated temperatures of up to 1200 °C is beneficial. Additionally, it has been shown that heated concrete's thermal performance is unaffected by a steel fiber concentration of 1%. The addition of steel fibers has a minimal impact on Poisson's ratio, resulting in a slightly higher value compared to the CS. The Poisson's ratio decreases as the temperature increases, eventually reaching insignificant values at a temperature of 1000 °C [50].

### **2.3.1 Application of Steel Fibers**

Steel fiber is used in many civil engineering structures. In-situ tunnel lining, road concrete, safety barriers, retaining walls, precast concrete, shotcrete, flooring, and bridges etc.



**Figure 2:** Steel Fibers.

**Table 3:** Properties of Steel Fibers.

Fiber length	24mm
E	195Gpa
Diameter	0.53mm
Aspect ratio	45
Tensile strength	2722Mpa

#### **2.4 High Strength Concrete**

ACI 363R-9200 [51] defines HSC as concrete with a compressive strength of at least 55 MPa. Compared to conventional strength concrete, HSC is more resilient and more robust. High-rise buildings are increasingly using HSC, which was previously more often used in projects like bridges, offshore constructions, and infrastructure projects. Columns are one of the principal applications of HSC in construction. [52]. High-strength concrete (HSC) may be effectively produced at various concrete plants by including refined additives, like silica fumes and water-reducing admixtures, in the context of HSC, the mineral admixtures often employed [32]. In high-strength concrete w/c ratio decreases and increases the binder content. To achieve the required workability superplasticizers are used. Silica fume is well recognized and mostly employed pozzolanas in construction. Its incorporation into concrete mixes leads to reduced levels of porosity, permeability, and bleeding. This is primarily attributed to the interaction between the oxides ( $\text{SiO}_2$ ) present in silica fume and the calcium hydroxides generated during the hydration process of conventional Portland cement. Pozzolanic reactions' main effects are decreased heat emission, increased strength, and a more compact pore size distribution [53]. The composition of HSC and NSC exhibits minimal distinctions,

with the primary differentiating factor being their structural behavior. Specifically, HSC and NSC differ in terms of their susceptibility to strength loss and explosive spalling. High-strength concrete (HSC) specimens exhibit a tendency to undergo explosive spalling, even when subjected to modest heating rates of 5°C/min or less.

## **2.5 Silica Fume**

Silica fume is defined in ACI 116R, “is very fine nanocrystalline silica produced in electric arc furnace as a byproduct of the production of elemental silicon or alloy containing silicon”. It is made up of very tiny round particles with a mean size of 4 to  $8 \times 10^{-6}$  inches as shown in Fig 3. The silica fume is dark grey. SiO<sub>2</sub> is colorless, the color is determined by iron oxide and carbon. The greater the carbon concentration, the silica fume becomes darker [54]. The findings of this study demonstrate that an increase in the proportion of silica fumes leads to a decrease in the workability of concrete. However, it also enhances the concrete's immediate mechanical characteristics, such as the 28-day compressive strength and secant modulus [53]. It enhances abrasion resistance, bond strength, compressive strength, reduce workability and protects rebar from corrosion.

- By using SF, toughness and bond strength can be increased.
- Abrasion resistance and durability is enhanced.

### **2.5.1 Uses of Silica Fume**

- Silica-fume shotcrete is a material that finds application in several engineering contexts, such as rock stabilization, mine tunnel linings, and the restoration of deteriorated bridge and marine columns, piles, and grouting for oil wells.
- Services for product repair A wide variety of cementitious repair treatments use silica fume [55].



**Figure 3:** Silica Fume.

### **2.5.2 Chemical Reaction of Silica Fume`**

Silica fume has a high degree of reactivity as a pozzolanic substance. It is because of high amorphous SiO<sub>2</sub> and extreme finesse. The role of silica fume in concrete may be examined through three fundamental mechanisms: Refining pore size and densifying the matrix by the reaction with free lime. Silica fumes react with free lime change orientation of CH to C-S-H and decrease thickness of ITZ. Compared to mortar made just of regular Portland cement, the addition of silica fume causes the thickness to be reduced. Additionally, there is a reduction in the degree of orientation of calcium hydroxide during the transition phase. Therefore, SF improves compressive strength and durability [55].

### **2.6 Testing Procedure Based on Loading and Heating Regime.**

Most test programs examining the deterioration of concrete's material characteristics at increasing temperatures employ one of three test methods: stressed, unstressed, or unstressed residual property tests. In the pre-heating step of the stress test, a load of magnitude equal to 40% of the member capacity is applied. The member is heated at a set pace until it reaches the specified temperature, at this point, it is maintained at that degree, and no additional heating is allowed. A complicated assembly of the furnace and loading equipment is required to perform tests under this loading and heating regime, in which the sample is placed in the furnace while the load is applied. Because unique preparations are necessary, it is a sophisticated system that is only sometimes found in structural engineering laboratories. This feature is usually found in laboratories dedicated to studying the fire characteristics of buildings. This loading and heating regime accurately depicts the real-life situation of structures in the case of a fire. Unstressed test circumstances are the second testing scenario. The specimen or part is not loaded in preheating circumstances in this case. In contrast to the stressed approach, the member or specimen is not loaded, and heating is administered at a controlled rate until the appropriate temperature is achieved. The temperature is then maintained consistently, and load is added at a predetermined pace until the structure fails. This heating and loading regime do not accurately represent the structural circumstances during a fire. Due to the lack of stressed test condition equipment, this testing condition is becoming increasingly essential. Although the findings obtained under unstressed test settings range in magnitude from those obtained under stressed test conditions, they

follow the same pattern, and the building under fire behaves similarly in each of these scenarios.

## **2.7 Previous Research on the Mechanical Properties of Concrete at High Temperatures.**

This section contains research papers that summarize flexural strength, modulus of elasticity, compressive strength, and mass loss at high temperatures. Heating rate, testing procedures (stressed, unstressed, or unstressed residual), size of the specimens, moisture content during heating, coarse and fine aggregates, strength (NSC or HSC), cement content, silica fume.

### **2.7.1 Compressive Strength**

Compressive test is a simple method of assessing concrete quality. In most of the grey structures, concrete is structurally active in compression. Although concrete is generally known for its ability to withstand fire, it is essential to note that its mechanical properties may still be significantly diminished. The compressive strength is mainly influenced by temperature [32]. concrete compressive strength under fire is dependent on several variables, including strength at standard temperature (NSC or HSC), nature of loading and heating regimen (stressed, unstressed, or unstressed residual), heating rate, aggregate cement ratio, w/c ratio, coarse aggregate type (normal weight siliceous and calcareous, or lightweight), and a variety of other variables [56]. The microstructure of high strength concrete (HSC) is compact and impermeable; vapor pressures caused by high temperatures generate tensile stress, resulting in unavoidable degradation in HSC compressive strength. HSC loses average strength up to 40% of its room temperature strength between 100°C and 450°C, while NSC loses 10 to 19% of its normal temperature strength. Recent research has revealed that both mixture I and mixture II of high-performance concrete can explosively spall. The phenomenon of explosive spalling occurred within a specific temperature range spanning from 240°C to 280°C [11]. With 250 and 350kg/m<sup>3</sup> cement dosages, they had room temperature compressive strengths of 28.16 and 48.99 MPa, respectively. After test specimens were subjected to five target temperatures: 100, 200, 400, 600, and 800 degrees Celsius, he looked at how compressive strength altered under unstressed residual conditions. The experiment's results point to a negative relationship between temperature and the remaining compressive strength of concrete, demonstrating that increasing temperature causes strength to decline. The compressive strength of the material decreased by

approximately 33 to 48% within the temperature range of 400 to 600<sup>0</sup>C. This decline in strength may be due to two main factors: the CSH gel's dehydration and the volumetric expansion caused by the conversion of Ca (OH)<sub>2</sub> to CaO. The specimens were heated to 800<sup>0</sup>c, which resulted in a considerable loss of strength. The experimental findings indicate that concrete decreases around 70% in residual compressive strength at escalating temperatures. [57].

When subjected to temperatures up to around 400°C, a strain-hardening cementitious matrix reinforced with hybrid fibers generally loses compressive strength by less than 20%. Nevertheless, when temperatures rise above this range, the rate at which strength diminishes also rises, resulting in a minimal retention of strength (less than 10% of the strength at average temperature) beyond 800-900°C [58]. Compressive strength falls as temperature rises, although additives may improve concrete's qualities while it's overheated [59]. The decrease in compressive strength of concrete after exposure to elevated temperatures was because of dehydration of hydrates of ettringite, CSH gel and the expulsion of capillary pore water [60]. The rate of heating and heating temperature also affects concrete properties subjected to elevated temperature and generate fractures in concrete. When concrete is heated to a temperature of 200°C or above, its compressive strength declines. When the temperature increases beyond the ambient level to 300°C, the breaking strength of concrete mostly stays constant or may even show a little increase. The compressive strength of concrete experiences a significant drop during the temperature range of 300 to 800<sup>0</sup>c. After reaching 800°C, most of the breaking strength of concrete has been destroyed [61]. The water vapor pressure caused by bound and free water due to elevated temperature causes cracks, which decreases the strength of concrete [13]. The initiation of micro-cracks increased permeability. The pore pressure within concrete exhibits a progressive increase over time as one descends further into its interior. This observation demonstrates that in the event of a first spalling, prolonged concrete exposure to increased temperatures will result in the accumulation of pore pressure over time inside the unaffected deeper areas. Consequently, this phenomenon will ultimately result in the occurrence of several instances of spalling throughout various levels of the concrete [7]. In comparison to normal temperature, the remaining compressive strength of high strength concrete drops to 20% and 40% at 200°C and 400°C, respectively. Concrete specimens heated to 400<sup>0</sup>c experienced severe degradation due to the breakdown of CH at temperatures over 350<sup>0</sup>c [9]. For unstressed

condition, compressive strength of high strength concrete samples was 65%, 67%, 53% and 37% at 100°C, 200°C, 400°C and 600°C consequently as compared to normal temperature [62]. Strength reduces with the increase in temperature and decreases more in smaller size samples. They also concluded that samples having air entrainment agent and fibers shows greater residual strength as compared to controlled specimens [63]. Silica fumes improve compressive strength by 19% and 25%. It is b/c SF chemically reacts with  $CA(OH)_2$  which forms CSH. The addition of cementitious materials, such as silica fume (SF), in concrete has been shown to be advantageous due to their ability to operate as effective fillers and undergo pozzolanic reactions. These reactions contribute to the development of a very compact microstructure in concrete containing SF. Therefore, the moisture content of concretes that have additional cementitious materials such as silica fume exhibits reduced permeability compared to OPC concretes [64]. At high temperatures, the transition zone and bonding between the aggregate and cement paste are poor due to contraction and expansion after being exposed to high temperatures, chemical degradation of the hydration product substantially reduced the strength of concrete. It was discovered that the three concrete samples' leftover compressive strengths were almost comparable after being heated to a temperature of 600°C. However, when comparing the relative residual compressive strengths, it was found that the concretes containing 6% and 10% SF exhibited reductions of 6.7% and 14.1% respectively, in comparison to the OPC concrete respectively, after exposure to 600 °C. The thick microstructure of concrete, which results in internal pressure from the transfer of the interlayer water to water vapor, is what causes the drop in strength for SF [64].

### **2.7.2 Flexural Strength Test**

Flexural strength is the capacity of a material to withstand deformation brought on by applied stress from outside. It is well known that concrete's flexural strength is much lower than its compressive strength [65]. Flexural strength, sometimes called modulus of rupture, bend strength, or transverse rupture strength, is a fundamental characteristic of a material. It is specifically defined as the stress that a material experiences immediately prior to yielding during a flexure test.

The volume fractions of the steel fibers added to the mixture were 0.5%, 1.0%, 1.5%, and 2.0%. Fiber-reinforced concrete's flexural strength improved by 126.6% at 2%. High

strength concrete under high loading develops cracks, the evenly distributed steel fibers in concrete composite block and arrest propagation of cracks [66]. SFRC has 3-81% higher flexural strength than control sample. Steel fiber significantly improves flexural strength in comparison to split tensile and compressive strength. As aspect ratio of steel fiber increases the relative flexural strength also increases [67]. The experimental findings indicate that the flexural strength exhibits an upward trend with a rise in the volume of fibers from 0% to 2%. This trend is observed irrespective of the replacement ratio of recycled aggregate, whether it is 0% or 100%. This finding implies a relationship between the number of fibers and the improvement in flexural strength provided by steel fibers, due to the possibility of increasing the flexural strength of reinforced concrete with additional cohesion (RAC) by the introduction of steel fibers [68]. The use of steel fibers enhances the flexural performance of hybrid Fiber-Reinforced Concrete (HFRC). Throughout the entirety of the loading procedure, the incorporation of steel fiber has been seen to substantially enhance both the bending stress and toughness of hybrid Fiber-Reinforced Concrete (HFRC). When the steel fiber volume content is increased from 0.5% to 1.5% in specimens with a polyvinyl alcohol (PVA) fiber volume content of 1.0%, the bending strength of HFRC significantly increases from 4.94 MPa to 7.39 MPa, demonstrating a considerable gain of 49.6%. Steel fibers are added to HFRC to increase its flexural strength and toughness via the process of bridge action, which stops fractures from spreading. The addition of extra fiber has little to no effect on the flexural properties of HFRC when the total fiber percentage surpasses 2.0%. [69]. With an increase in temperature, the MOR decreases more quickly than compressive strength. Tensile strength of concrete is more sensitive than compressive strength because of the development of micro and macro fractures [58].

The results of this research show that adding basalt fibers to composites significantly improves their tensile strength, flexural strength, and toughness index. It is important to note, nevertheless, that there was no appreciable increase in compressive strength [26]. The ultimate flexural capacity of basalt macro fibers concrete beam is improved as compared to control beam with no fibers. However, by adding BF into concrete beam have maximum deflection at failure than corresponding beams with no fibers [70]. According to the experimental results, adding basalt fibers at a concentration of 0.25 percent significantly increases flexural strength compared to the control sample.

Furthermore, it was noted that concrete with a 1% fiber content had enhanced strength. This was evidenced by residual strength gains of 94.2% and 64.96% when subjected to 300°C and 600°C, sequentially. Additionally, the basalt fibers form a network within the concrete and that's why concrete withstands high stress [12]. Concrete having basalt fibers fail is same brittle failure as conventional concrete and no bridging phenomena was observed [38]. The user has provided a numerical reference. The inclusion of 0.5% fibers in basal fiber reinforced concrete had a notable improvement of 7.32% in its flexural strength. The enhanced strength of concrete is due to the stabilizing effect of short fibers, as well as the presence of high elasticity and high tensile strength. The basalt fibers act as a medium for transmitting stresses at elevated temperatures, and because of the fibers' weakening, further stresses are released. When exposed to temperature conditions, the remaining strength of BFRC displays higher values compared to standard concrete. The specimens' flexural fractures, both those with and those without fibers, are quite distinct. As the number of chopped fibers increased, the flexural strength increased as well. The inclusion of a 1.5% by total volume of mix of BF content resulted in significant enhancements in the flexural strength of various types of aggregates. Specifically, the flexural strength of natural aggregate improved by 74.55%, untreated recycled concrete aggregate had a 61.45% rise, and treated RCA exhibited the highest improvement of 82.65% [71].

### **2.7.3 Elastic Modulus**

The stress-strain connection is measured by the modulus of elasticity, which is a crucial factor in determining how concrete deforms in response to operating loads [72]. The attribute that was most negatively damaged, according to the analysis of the remaining mechanical parameters, was the modulus of elasticity. This phenomenon is commonly observed in concrete subjected to extreme temperatures [9]. The modulus of elasticity of different types of concrete at ambient temperature falls within the range of  $5 \times 10^3$  to  $35 \times 10^3$  MPa. This value is affected by several variables, including the w/c ratio, life of concrete, and the kind and number of aggregates used. Although there is a noticeable amount of variation in the stated test results, both forms of concrete show a similar trend of decreasing elastic modulus as temperature rises. The presence of excessive thermal stresses and physical and chemical changes in the concrete's microstructure may be blamed for the drop in modulus seen in both NSC and HSC [73]. The results of a previous study indicate that the elastic modulus of HSC under fire may not be

significantly affected by the addition of SF. However, it is highlighted that the selection of aggregate variety has a more significant influence on the final strain of HSC [32]. Higher temperatures cause the basalt fibers to soften, which reduces their brittleness. However, when subjected to high temperatures, elastic modulus in the specimens with BFRC decreased in a manner like that seen in the specimens without fibers. The decomposition of hydration products is responsible for the reduction in stiffness and elasticity modulus. The filler effects brought on by the presence of short fibers, the crack-bridging properties demonstrated by these fibers, along with their excellent tensile strength and elasticity, are the main factors that contribute to the increase in strength of BFRC [12]. The addition of PP fiber to FRC did not improve the residual elastic modulus. Furthermore, the influence of fiber dose and fiber type became negligible beyond 600°C. The overall behavior of the concrete remains consistent regardless of the proportioning of PP-F and/or S-F fibers [74]. When comparing the different mixes, it was observed that the mixes containing 1% steel fibers exhibited a superior preservation of the elastic modulus compared to the concretes created with PP fibers or a mixture of PP and steel fibers. As the temperature rises, the loss of compressive strength is greater than the decline in elastic modulus [75]. The inclusion of fibers did not alter the observed relationship between the modulus of elasticity and temperature. Fiber-reinforced concrete (FRC) that incorporates both polypropylene and steel fibers exhibit an 8% increase in modulus of elasticity as compared to normal concretes. The reduction in residual modulus of elasticity is comparatively less pronounced in FRC as compared to non-FRC specimens. This effect is particularly evident at a temperature of 750°C [76]. Concrete's secant modulus rises when silica fume replacement amount is raised [53]. The elastic modulus of elasticity of RAC at room temperature and after exposure to 200°C decreases with increasing steel fibers, but for specimen elastic modulus increases with inclusion of steel fibers after exposure to 400°C and 600°C the most significant effect on elastic modulus when steel fibers 1.5% [45].

#### **2.7.4 Stress-Strain Compressive Curve**

Concrete stress-strain compressive response is critical since it is a required input parameter in mathematical models that anticipate the reaction of a concrete structural element. To model the response of a concrete structural section exposed to fire using a numerical technique such as finite element modeling, a constitutive model of concrete must be provided that can capture the strains at various stress levels and temperatures.

Compressive stress-strain curve in reactive powder concrete exhibits similarities when subjected to temperature variations, particularly in relation to varying steel fiber contents. At 300°C, the shape of the stress-strain curve exhibits minimal deviation from its initial unheated form. As temperatures escalate to the range of 300–700°C, there is a noticeable flattening of the stress-strain curves along with a downward and rightward shift in the position of the peak points. Upon subjecting the concrete to temperatures between 800–900°C, the peak points demonstrate a tendency to shift upwards and leftwards once more [77]. After exposure to a temperature of 600°C, the concrete specimens' average strain at the peak of tension is almost 4.8 times higher than that of the unheated concrete specimens. In the context of recycling aggregate Concrete (RAC), it is often observed that a concrete mixture containing a larger proportion of steel fibers tends to exhibit a little greater strain at the point of maximum stress especially at 400°C and 600°C [45]. Under unstressed circumstances, a study was conducted in which the stress-strain response of HSC mixtures containing FA was measured. The temperatures exposed were 250°C, 450°C, 550°C, 650°C, 750°C, and 850°C, with a rate of heating was 2°C/min. For capturing the stress-strain response, they used a strain-controlled approach. The cylinders were 80 x 300 mm in size and had a compressive strength of 91.8 MPa at room [78].

# **CHAPTER 3**

## **EXPERIMENTAL PROGRAM**

### **3.1 General**

The HFRC (basalt and steel fibers) at elevated temperature needs a detailed test program with various concrete mix regimes. The test thesis will include compressive and flexural strength tests, Post crack energies, stress strain graphs, elastic modulus, Pre-crack energies, toughness index, and mass loss. Various authors have explored high strength concrete in depth in the literature, but there is no one set of studies that covers the mechanical characteristics of steel and basalt fibers intruded in concrete at high temperature. To understand the fire and spalling behavior of concrete, basic mechanical tests namely flexural and compressive test, stress strain curve, elastic modulus, and mass loss are performed at temperatures of 23°C, 300°C, 600°C and 800°C under residual test conditions. The details about the test program and procedure, materials and mixed regime are discussed in this chapter. The mechanical and material qualities that were assessed are provided in graphical form, and the data obtained was also compared with control mixtures. This chapter presents the details about the materials, methods and procedures used in this study. All mechanical and material parameters that were investigated were graphed, and the produced data was compared to control mixtures.

### **3.2 Formulation of Experiments for Material Properties**

The test program was carried out elevated temperature material property tests on all five formulations of concretes. Cylindrical specimens of dimension (300mm height x 150mm diameter) along with small beam specimens of dimension (100mmx100mmx400mm) were fabricated from each batch of concrete mixes, at 28-days of curing these specimens were then subjected to escalating temperatures from 23°C-800°C. The compressive strength tests were conducted according to the ASTM C-39 standard, whereas the flexural strength testing was according to ASTM C293/C293M-16 standard. The study employed the residual test method to investigate the mechanical and material characteristics of the mixtures at different exposure temperatures.

### 3.3 Materials

#### 3.3.1 Cement

OPC Type-I” Cherat cement limited,” according to ASTM C150 [79], is used as a binder.

**Table 4:** Raw Ingredients of Cement.

Item	Percentage of Oxides by weight
CaO	63.52
SiO <sub>2</sub>	21.23
Al <sub>2</sub> O <sub>3</sub>	5.55
Fe <sub>2</sub> O <sub>3</sub>	3.23
SO <sub>3</sub>	2.54
MgO	0.92
K <sub>2</sub> O	0.63
Free Lime	0.54
Na <sub>2</sub> O	0.14

#### 3.3.2 Fine Aggregates

The fineness modulus of fine aggregate was 2.62 and obtained from the river. Furthermore, the results for grading and standard (ASTMC33/C33M-13 2013) [80] are presented in [Table 6](#) mentioned below. Fine and coarse aggregate properties are mentioned in [Table 5](#) below.

**Table 5:** Properties of Aggregates.

Aggregate type	Coarse aggregate	Fine aggregate
Specific gravity	2.68	2.43
Fineness modulus	7.29	2.61
Water absorption	0.69%	1.19%
Max size of aggregate	12.5mm	--

**Table 6:** Gradation of Fine Aggregate.

Sieve No	Sieve Sizes (mm)	Retained Weight (gm)	Percentage retained	Cumulative % retained	Percentage Passing	ASTM Lower Limit	ASTM Upper Limit
#4	4.75	8	1.64	1.63	98.36	95	100
#8	2.36	35	7.17	8.81	91.19	80	100
#16	1.18	73	14.6	23.7	76.3	50	85
#30	0.6	128	26.22	50	50	25	60
#50	0.3	170	34.83	84.83	15.17	5	30
#100	0.15	74	15.16	100	0	0	10
Total		488					
(gm)							

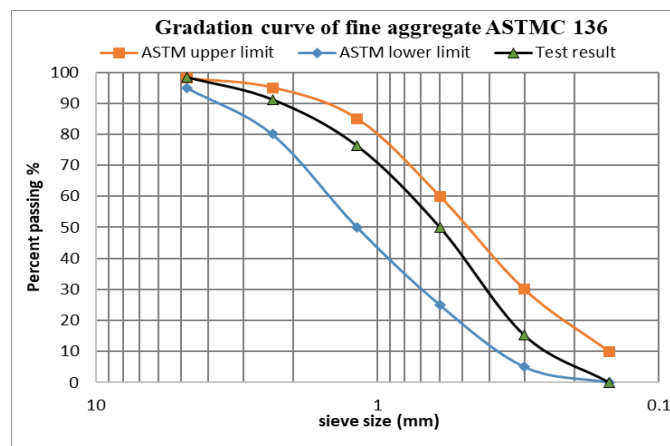


**Figure 4:** Gradation Curve of Fine Aggregate and ASTM Lower and Upper Limits.

### 3.3.3 Coarse Aggregates

The coarse aggregate, with a maximum size of 12.5 mm, was employed under saturated surface dry conditions. The coarse aggregates' physical properties are summarized in Fig 5, and their gradation is listed in Table 7 below.

**Table 7:** Gradation of Coarse Aggregate.

Sieve No	Sieve Sizes (mm)	Retained weight (gm)	Percentage retained	Cumulative % retained	Percentage Passing	ASTM Lower Limit	ASTM Upper Limit
1.5	38.1	0	0	0	100	95	100
1	19.08	160	3.18	3.18	96.82	80	100
0.75	12.7	350	6.37	9.56	90.08	50	55
0.5	9.525	1915	37.22	47.13	52.86	30	35
0.375	4.76	1200	23.32	70.45	29.54	5	20
0.1875	25.4	1520	29.54	100	0	0	0
pan		0					
Total (gm)		5145					

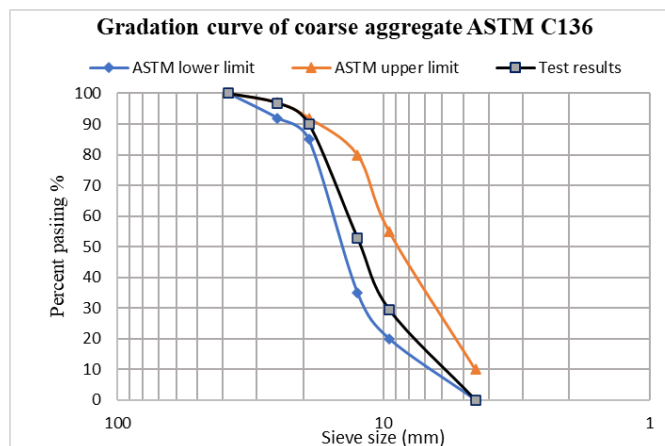


**Figure 5:** Gradation Curve of Coarse Aggregate and ASTM Lower and Upper Limits



**Figure 5:** Sieve Shaker.

### 3.4 Admixture

#### 3.4.1 Super Plasticizer

High-performance water-reducing admixtures were added to improve concrete quality at a low w/c ratio. The carboxylic acid derivative-based chemical admixture was used. Superplasticizer chemorite-303SP was used as water water-reducing admixture with ASTM C494-19 [81]. It was obtained from the chemical supplier IMPORIENT Chemical (PVT) LTD.

**Table 8:** Chemical Properties of Superplasticizer.

composition	Carboxylic acid derivative
Form	Whitish pale liquid
Density at 25 <sup>0</sup> c	1.06±0.01kg/lit
Chloride content	Nil (EN 934)
Storage life	Minimum 12 months

#### 3.4.2 Silica Fume

The research's mineral admixture used is Densified Silica Fume. This densified silica fume has a very high density and average particle size, leading to the improved microstructure of the resulting concrete. It is particularly suitable for mixing concrete where concrete must resist sulfates and chloride from the surrounding environment. It was obtained from the chemical supplier IMPORIENT Chemical (PVT) LTD. Chemical admixture having ASTM C1240 [82].

**Table 9:** Properties of Silica Fume.

Appearance	Grey powder
size	0.5 μm
Dry density	450 kg/m <sup>3</sup>
Specific surface	15-30 m <sup>2</sup> /g
Specific gravity	2.2-2.3
Storage life	Minimum 24 months

## **3.5 Fiber Additives**

### **3.5.1 Importance of Fibers**

FRC has shown to be quite effective in various applications, like slabs on grade, shotcrete, architectural and design panels, prefabrication products, offshore platforms, constructions in seismic zones, thick and thin repairs, crash barriers, foundations, and hydraulic structures. Fibers might enhance the characteristics of concrete if they are added to it. The fundamental vulnerability of ordinary concrete arises from microscopic fissures located at the contact between the mortar and aggregate. FRC is a composite material made mostly of conventional concrete with fine fiber reinforcement. Fibers are crucial in mitigating fracture formation by enhancing the mechanical properties of inherently brittle materials like cement concrete, which typically exhibit poor tensile strength and impact resistance. The resulting composite material gains improved crack resistance, enhanced flexibility, and distinctive post-cracking behavior prior to ultimate collapse by including fibers.

### **3.5.2 Steel Fiber**

This research study utilized 24 mm long fibers with an aspect ratio of 45. The fibers' diameter was 0.559 mm, and density was 7.85g/cm<sup>3</sup>. Its melting point is about 1700<sup>0</sup>c.

### **3.5.3 Basalt Fiber**

Basalt fibers (BFs) were ordered from Jiangsu Horyen International Trade Shanghai, China. It is manufactured at a temperature of 1500-1600<sup>0</sup>c.

## **3.6 Mix Proportions.**

One experimental group consisted of a high-strength concrete (HSC) formulation. In contrast, the other experimental group consisted of four modified high-strength concrete formulations that contained SFs and BFs with varying percentages (0.25% HFR-HSC, 0.5% HFR-HSC, 0.75% HFR-HSC, 1% HFR-HSC) were prepared. In this hybrid fiber reinforced concrete, both SFs and BFs are added in equal proportion by percentage, like in 0.25%, half percentage of steel fibers and half of basalt fibers were added. Steel fibers have high density, so the quantity of steel fibers was higher than basalt fibers. All mixes are made with a low w/c ratio of 0.35, with plasticizer by 1 percent by weight of cement. After 24 hours, the samples were de-molded and put in a water tank for 28 days. To analyze the strength evolution of formulations, compressive strength tests were done

according to ASTM C39 [83] and flexural test was according to ASTM C293/C293M-16 [84].

**Table 10:** Mix Design in Kg/m<sup>3</sup>.

Mix ID	CM	FA	CA	Sf	Water	SP	%	
							BFs	SFs
HSC	440	627	1253	44	154	4.39	0	0
HFRC-0.25%	440	627	1253	44	154	4.39	0.125	0.125
HFRC-0.5%	440	627	1253	44	154	4.39	0.25	0.25
HFRC-0.75%	440	627	1253	44	154	4.39	0.375	0.375
HFRC-1%	440	627	1253	44	154	4.39	0.5	0.5

**Note:** CM (cement), FA (fine aggregate), CA (coarse aggregate), Sf (silica fume), SP (supper plasticizer), BFs (basalt fibers), SFs (steel fibers)

### 3.7 Sample Preparation

For each kind of formulation, concrete samples with dimensions of 150 x 300 mm were cast in the cylinders, and 100 x 100 x 400 mm were cast in the case of beam specimens for each temperature variation 03 sample and before casting cylinders and prism beams, applied oil on their inner surface to have a smooth surface of samples. The concrete specimens were allowed to remain within the molds for 24 hours after pouring. Samples were carefully molded and placed in water tanks for 28 days in a controlled environment of 13<sup>0</sup>c. Compressive and flexural strength tests were conducted at 28 days.



(a)



(b)

a) Oiling of the internal surface of molds. It was done 24 hours before casting specimens. The primary purpose of it was to have a smooth surface of cylinders. (b) small amount of steel and Basalt fibers were added after the addition of coarse aggregates into the mixer



(c)



(d)

(c) Hybrid fibers were added in small proportions after adding fine aggregate. (d) Hybrid fibers were added in small amounts after cement. Avoid voids and spread equally in the mix to prevent the balling effect.



(e)



(f)

(e) concrete specimens after casting. f) Concrete samples in a curing tank for 28 days.

**Figure 7:** Mixing, Casting and Curing of Concrete Specimens.

**Table 11:** Overview of Cylinders and Beams Samples with Temperatures.

Temp	Mix Type					Cylinders	Beams
	CS	HFRC-0.25%	HFRC-0.5%	HFRC-0.75%	HFRC-1%		
23 <sup>0</sup> C	2	2	2	2	2	10	10
300 <sup>0</sup> C	2	2	2	2	2	10	10
600 <sup>0</sup> C	2	2	2	2	2	10	10
800 <sup>0</sup> C	2	2	2	2	2	10	10
						Total = 40x2= 80	

A total of 40 cylinders and 40 prism beams were cast for residual testing at elevated temperatures. Two concrete specimens were designated for high temperature material property tests at each target temperature. Before residual test all cylinders were capped with gypsum mortar [85].

### **3.8 Material Property Tests**

The mechanical properties testing was conducted on heat-treated samples in their residual state. The material property tests were assessed, including compressive and flexural strength, stress-strain curve, elastic modulus, and mass loss. This section briefly discusses the testing approach and technique, testing equipment, testing variables, and fire loading characteristics.

### **3.9 Fire Loading Characteristics**

Two main fire-loading factors influence the test findings of samples subjected to high temperatures. Heating rate and targeted temperatures. Due to a lack of suitable higher-temperature testing standards, these two properties were chosen based on previous research on concrete specimens at high temperatures.

### **3.10 Target Temperature, Heating Rate, and Hold Time for Test Method.**

The most frequently used target temperatures are 23°C, 300°C, 600°C and 800°C. Types of aggregates significantly impact concrete fire response as calcareous aggregates tend to dehydrate at 800°C. This temperature, i.e., 800°C is also selected for the study of microstructure and crack pattern analysis. To assess the mechanical characteristics of concrete at elevated temperature conditions, the heating rate used by several researchers lies in the range of (2-5°C)/minute. The heating rate varies in case of a realistic fire; sometimes the elevation rate may rise to 25°C/min [86]. This study carefully determined a constant rate of 5°C/min. In this study, samples were tested at target temperatures 23°C, 300°C, 600°C, and 800°C. When subjecting a concrete sample to heating in an electric furnace, the temperature of the furnace rises at the specified rate. A proper hold time must be supplied to the sample under heat treatment to achieve a thermal steady state. A thermocouple was used to detect the core temperature of specimens. It is simply wire. The k-type thermocouple was used for this purpose. A hole was created from one of the cylinder's round ends, a thermocouple was placed, and then cement paste was grouted into the hole and left to set. All the mixes were given a suitable hold time

according to thermocouple values to achieve a thermal steady state [87]. The data recorder was then equipped with thermocouples to measure the temperature record over time. Then, the thermocouple cylinder was placed within the heating chamber, which was heated to the desired temperature. The temperature data was measured about time and plotted accordingly. The samples were kept for two hours after the target temperature to achieve both core and furnace temperature thermal stability. It is clear from the above that the control concrete cylinder's core takes 2 hours and 25min to attain 300<sup>0</sup>C temperature, 3 hours, and 26 minutes to attain 600<sup>0</sup>C, and 4 hours and 55min to attain 800<sup>0</sup>c. The core temperature of samples containing SF-BF 0.25% reaches 300<sup>0</sup>c at 2 hours and 22 min, 3 hours and 23 min to achieve 600<sup>0</sup>c. The core temperature of samples containing SF-BF 0.5% reaches 300<sup>0</sup>c at 2 hours and 19 min, 3 hours and 15 min to attain 600<sup>0</sup>c.

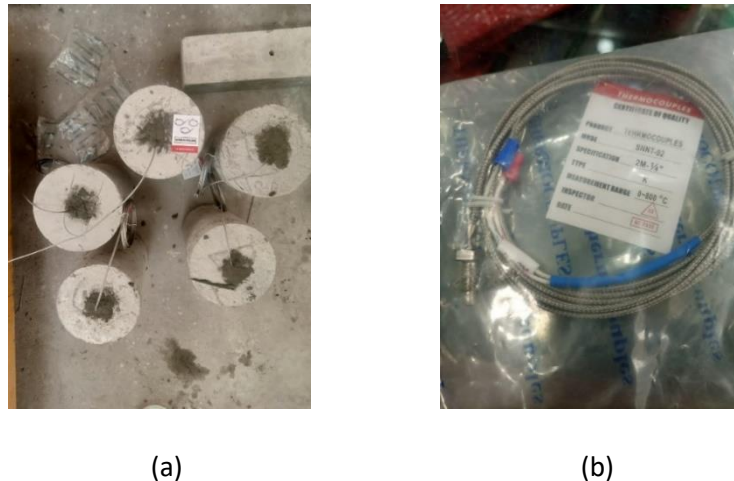
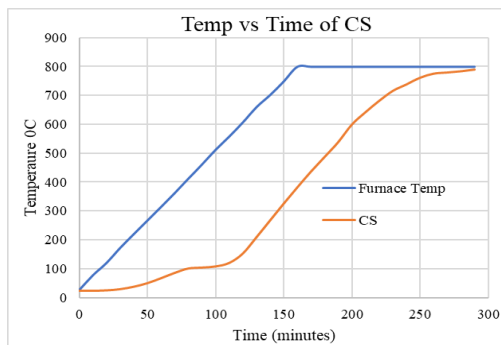


**Figure 6:** K-Type Thermocouples Drilled Inside the Specimen.

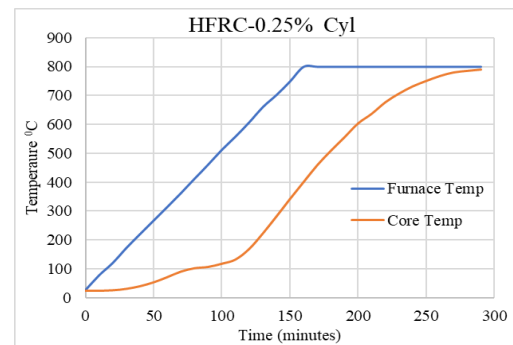
### 3.11 Test Apparatus and Procedure

According to [ASTM-C39](#) and [ASTM C239/C239M-16](#), the specimens' compressive and flexural strengths were evaluated. A controlled loading rate of 0.2 Mega Pascal per second was used to create the stress-strain curves. The stress-strain results of the response curves were also used to calculate the modulus of elasticity based on the specified variables. A furnace with a 1200 °C capacity was utilized for temperature control, and a computerized temperature-time controller was placed in the furnace to regulate time and maintain the necessary conditions. K-type thermocouples were inserted into the core of a typical sample to monitor temperature changes and guarantee that concrete specimens were receiving a balanced dispersion of heat. During the testing, temperature measurements for representative samples were obtained, which helped

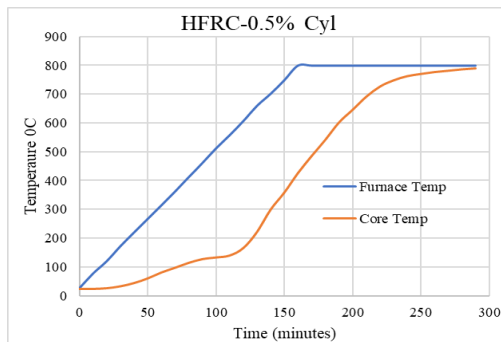
determine the required hold time and heating rate by RILEM test guidelines (“Recommendation of RILEM TC 129-MHT ‘Test Methods for Mechanical Properties of Concrete at High Temperatures’ Modulus of Elasticity for Service and Accident Conditions,” 2004). The samples were heated to the required temperatures at a regulated rate of 5°C/min. Based on temperature-time graphs, a hold duration of 2.5 hours (150 minutes) was prescribed to maintain thermal equilibrium (stationary state) conditions. The specimens were allowed to cool down to the ambient temperature to reduce the effects of heat shock. The targeted temperatures were 23°C, 300°C, 600°C, and 800°C, sequentially. To determine mass loss, the mass of every sample was counted both before and after the fire exposure. Record initial temperature note time after five minutes note final temperature. It was calculated that the rate of cooling was 6<sup>0</sup>c/min.



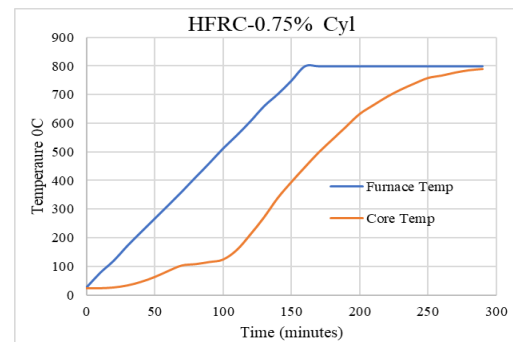
(a)



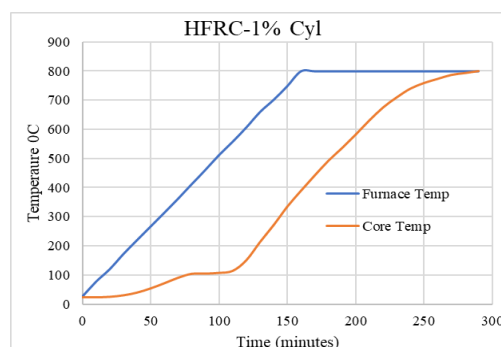
(b)



(c)

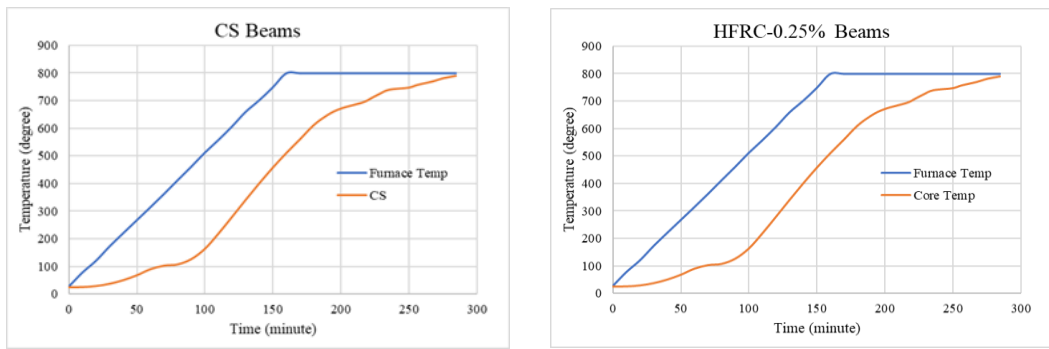


(d)



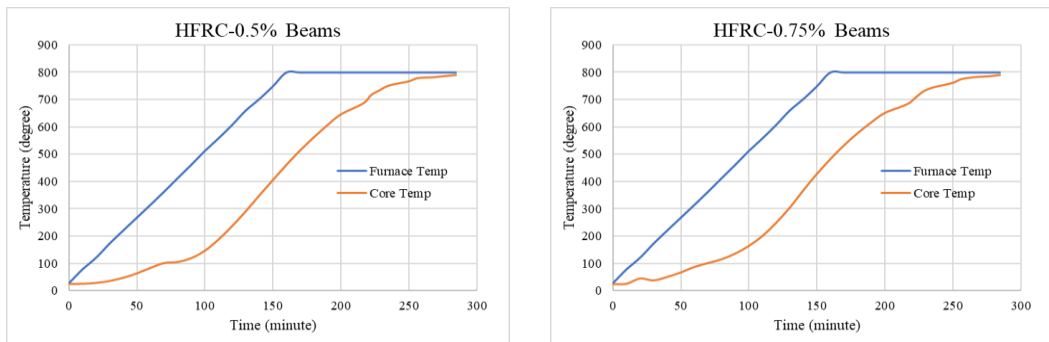
(e)

**Figure 9:** Temperature Vs Time Graphs of Cylinders.



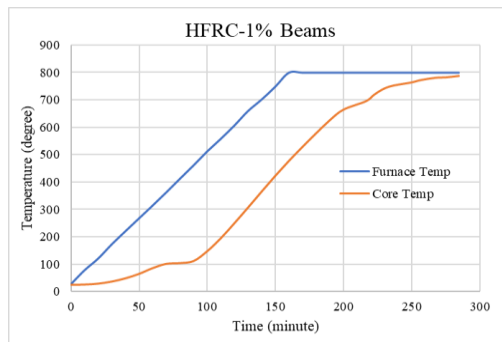
(a)

(b)



(c)

(d)



(e)

**Figure 7:** Temperature Vs Time Graph of Prism Beams.



**Figure 8:** Electric Furnace for Heating the Samples to Targeted Temperatures.

### 3.11.1 Compressive Strength Test

After being heated to the required temperature, the specimens were allowed to cool until they reached a state of thermal stability. Since there are no published testing standards for high-temperature compressive testing of concrete specimens, the ASTM (ASTM C39/C39M-16b 2016) testing method for room temperature is used to evaluate the compressive strength of the concrete at the appropriate temperature ( $f_c'$ , T). The compression loading rate was 0.2Mpa/sec [83] and tested two cylinders at each target temperature.



**Figure 9:** Compression Testing Machine.

### 3.11.2 Flexural Strength Test

Flexural strength is often used as a substitute for tensile strength. Alternately, the computation of the extreme fiber stresses brought on by the bending moment may be utilized to calculate the modulus of rupture while bending a part. The load was delivered to the specimen steadily to keep it under constant and shock-free pressure. 0.9 to 1.2 MPa per minute [125 and 175 psi per minute] of the load will be applied to the tension face each minute [84].

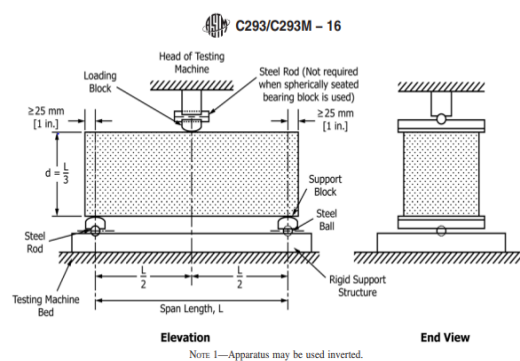


**Figure 10:** Flexural Test Assembly ASTM C (293/293-16).

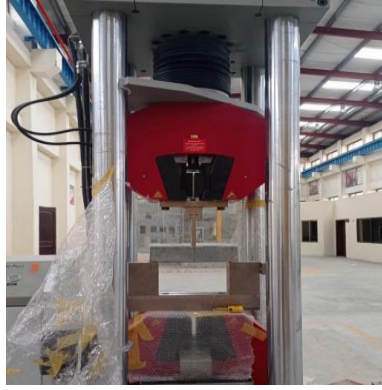


**Figure 11:** Universal Hydraulic Testing Machine for Flexural Strength Test.

### 3.11.3 Stress-Strain Curve

While performing compression tests, the stress-strain response of concrete specimens was captured using a data-collecting system. The rate of loading was kept at 0.2Mpa/sec till the failure. Load and deformation data were obtained using a load data gathering system connected to a universal testing machine and LVDTs. Based on the load deformation response, the stress-strain curve was plotted at the desired temperatures.

### 3.11.4 Modulus of Elasticity (E)

concrete specimens were evaluated using the stress-strain curves with a relationship described in ASTM C469 [88].

### 3.11.5 Mass Loss

Concrete samples were first weighed before being heated to determine the mass loss. Subsequently, the specimens were heated to a predetermined temperature and allowed to cool down to the ambient temperature. Later, the specimens were reweighed using a precision weighing scale to measure to a minimum resolution of 0.001 grams. The following relationship was used to compute relative mass loss at a specific temperature.

$$M_{T,loss} = \frac{\text{Mass at target temperature}}{\text{Mass at room temperatuer}} = \frac{M_T}{M}$$

# CHAPTER 4

## RESULTS AND DISCUSSIONS

### 4.1 General

This chapter summarizes and analyses the results of tests done on concrete specimens, including mass loss, mechanical properties, and compressive failure mode, and visual observations were taken to determine how the color and surface cracking of samples changed after they were removed from the electric furnace. The resulting mechanical properties data for HSC and modified HSC with steel fibers and basalt fibers at different percentages are used to construct relationships for various material properties as a function of temperature spanning from 23 to 800 °C.

### 4.2 Elevated Temperature Mechanical Properties

#### 4.2.1 Compressive Strength

The compressive failure load of the samples was measured at various temperatures, as shown in Fig.15, showing that residual compressive strength varies with temperature in terms of both absolute and relative values.

The compressive strength of concrete decreases with increasing temperature shown in Fig (15), namely in control (HSC), 0.25% HFR-HSC, 0.5% HFR-HSC, 0.75% HFR-HSC, and 1% HFR-HSC, due to hydrothermal impacts, such as the loss of water and chemical changes that occur within the concrete matrix [89]. A noticeable difference occurs by removing adsorbed and free water, resulting in increasing pore pressure, which continues till 300<sup>0</sup>c [90], further increase in temperature to 400°C, and decomposition of C-S-H and CH occurred, which caused a significant loss of strength [8]. The changes above the threshold of 500<sup>0</sup>c are dramatic and irreversible [91]. Moreover, an essential factor contributing to the decline in strength at 600°C is the thermal instability of aggregates, which is caused by the de-carbonation process of limestone taking place within the temperature range of 600-800°C [92]. Modified HSC samples surpassed control samples, especially b/w 200<sup>0</sup>c and 600<sup>0</sup>c. Modified HSC basalt fibers decrease thermal stress by reducing pore pressure, while steel fibers bridge the fissures arising from hydrothermal changes. The inherent ability of basalt and steel fibers to bridge cracks has maintained the integrity of the load-bearing area, hence improving the strength retention. This characteristic facilitates the homogeneous dispersion of thermal loads and mitigates the heat transmission between the exterior

surface and concrete interior. Later, lower tensile stresses and thermal cracking are generated. Due to the basalt and steel fibers' anchoring properties, fracture development was reduced. Thermal fractures decreased compressive strength in the absence of this mechanism in the control sample (HSC).

The incorporation of hybrid fibers into HSC samples resulted in an improved microstructure of the specimens, leading to a higher compressive strength at ambient conditions up to 4.39%, 22.41%, and 9.61% for (0.25%-HFRC, 0.5%-HFRC and 0.75%-HFRC), respectively, in comparison to control specimen, further increase to 1% HFRC strength decreases to 4.25% from the reference sample. As the fiber increases, the compressive strength of modified samples increases, and maximum strength achieved at 0.5% hybrid fibers reinforced concrete. However, beyond 0.75% fiber addition then strength reduction occurs which is due to agglomeration of fibers, non-uniform distribution of fibers, and formation of pores, which causes the formation of weak zones within concrete. When fibers increase beyond optimum level, then upward trajectory of entrapped air was observed [93]. Additionally, their reduced stickiness with cement paste may also decrease strength [94]. At room temperature, the specimen reaches its maximal strength. When exposed to a temperature of 300<sup>0</sup>c, the specimens' strength significantly decreased. At this temperature concrete with 0%,0.25%, 0.5%, 0.75% and 1% addition of hybrid fibers the strength reduction was 32.55%, 28.08%, 24.95%, 25.35% and 33.9% respectively. Interfacial bonding in the region between cement paste and aggregate is lost because of internal water evaporation [95],[96]. Stress induced by evaporation pressure over 400<sup>0</sup> c resulted in the disintegration of C-S products [97]. At 600<sup>0</sup>c strength reduction were 49.09%, 46.42%, 44.71%, 42.21%, 52.23% respectively. Around 400-600<sup>0</sup>c a notable amount of C-S and C-S-H product decompose, that's why rapid strength loss occurs [98]. However, the hybrid modifier samples show better retention of strength as compared to control specimen. The specimen containing 0.5% fibers exhibits the best strength preservation, followed by 0.75% and 0.25%, it may be attributed to the superior heat-resistant material incorporated in the matrix. The thermal stress, which is directly related to the characteristics of the microstructure of concrete, may be responsible for the loss in compressive strength. The specimens composed of basalt fibers exhibited significant resistance against spalling and steel fibers resist cracking at macro level. At 800 <sup>0</sup>c concrete with 0%, 0.25%, 0.5%, 0.75% and 1% hybrid fibers (HF) strength were

reduced to 85.08%, 84.43%, 84.43%, 83.74, and 86.94%. It was observed that at 600 °c the concrete with 0.75% HF strength reduction was lesser than others. When concrete cylinders were heated to high temperatures, the presence of steel fibers significantly reduced the rate at which the cylinders disintegrated completely. After being subjected to a compression test, the cylinders' structural integrity is improved according to the quantity of steel fibers that are present in the material. In addition, the fracture will often become more dispersed and zigzag-shaped as the proportion of steel fiber in the material increases. The strength decreased beyond 0.75%, possibly related to a weak contact between the fibers and the cement. The heterogeneity of the mixture, which results from a greater amount of hybrid fibers, may be responsible for the observed decrease in compressive strength. This heterogeneity, in turn, reduced the amount of cement utilized. Moreover, the robust connection provided by fibers and their increased resistance to being pulled out contribute to the enhancement of characteristics [99], [96].

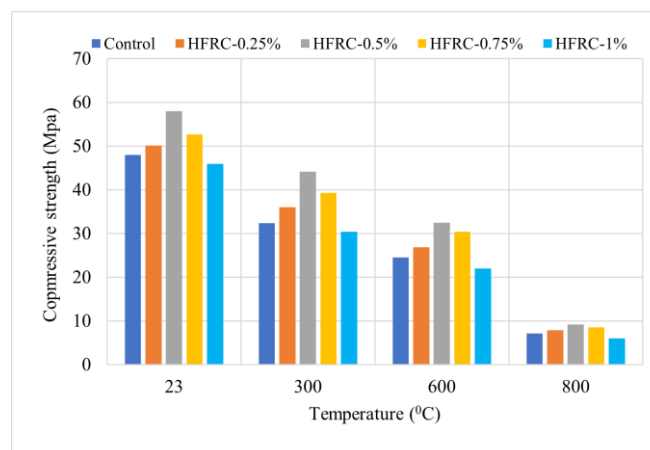


**Figure 12:** Variation of Compressive Strength as A Function of Temperature.

#### 4.2.2 Stress-Strain Curve

The cylinder specimens were [150x300mm] in accordance with ASTM C-39. The stress-strain curve for each specimen was created by performing compression tests on cylinders at a constant loading rate of 0.2 MPa/sec, as was explained earlier. The significant features associated with the stress-strain curves, such as compressive strength, elastic modulus, post-fracture energy, and compressive toughness, were derived by averaging the results from three specimens with the same composition.

The experimental findings demonstrate that the incorporation of HF leads to a notable change in the stress-strain curve. Specifically, the branch of the curve that is going downwards becomes more flattened when a concrete mixture contains hybrid fibers.

The flattened curve after peak stress indicates that by addition of fibers change brittle to ductile behavior. It is common for the initial slope of the stress-strain curve to decrease as well as the compressive strength of a material when it is subjected to elevated exposure temperatures. The stress-strain graphs at ambient temperature for HFR-HSC show ductile behavior with superior peak load and peak strain than CS. The increased post-peak phase shown by these graphs suggests an enhanced capacity to absorb energy, as shown in [Fig 17](#). The high-temperature effect reduced both maximum stress and peak strain for all combinations of concrete mixture compared to the specimens tested at room temperature. When fiber content increased from 0.25% to 0.75%, the peak stress of HFRC was more than CS at room temperature; beyond the 0.75% addition of HF, the peak stress decreased by 4.25%. The previous study likewise revealed a higher maximum stress when steel fibers were added in the HFRC [99]. Moreover, the increased peak stress of HFRC can be related to the incorporation of basalt fibers at different concentrations. The literature also reported the optimize peak stress with a 0.15% basalt fiber content in concrete [101]. The superior mechanical capabilities exhibited by basalt fibers, along with their excellent compatibility with cement matrices, have led to the notable improvement in peak stress observed in composite matrix [102]. The peak stress of concrete having 0.25% basalt fibers was also observed by researcher [12]. Ultimate strain also increases with increasing fibers content. The observed enhancement in the strain capacity of HFRC demonstrates a beneficial synergistic effect comparable to that of CS. The stress-strain curves demonstrate that the area beneath them increases as the dosage of steel fibers increases. This indicates that a higher content of steel fibers leads to improved ductility and toughness [77]. Similarly steel and basalt fibers in concrete offer bridge effect after peak load, that's why area under stress-strain curve increases. In addition to proper bond b/w HF and concrete matrix enhance peak stress and ultimate strain [41]. In contrast, steel fiber can only successfully stop fractures from spreading at the macro level, while basalt fiber can effectively stop cracks from spreading at the meso level, as depicted in [Figure 16](#), certain portions of basalt fiber contribute at the micro level. Moreover, the incorporation of hybrid fiber into concrete results in enhanced residual strength when exposed to fire, mostly due to its confinement mechanism. Up to 300<sup>0</sup>c, there was little difference between the HFRC-0.5% and HFRC-0.75% formulations in terms of the retained strength. This can be seen in [Figure 17 \(c\) and \(d\)](#).

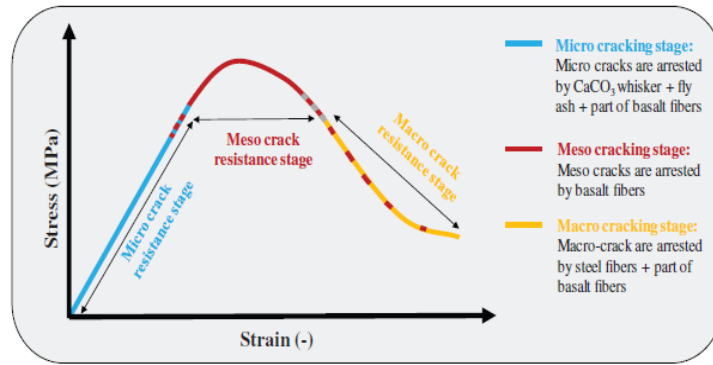
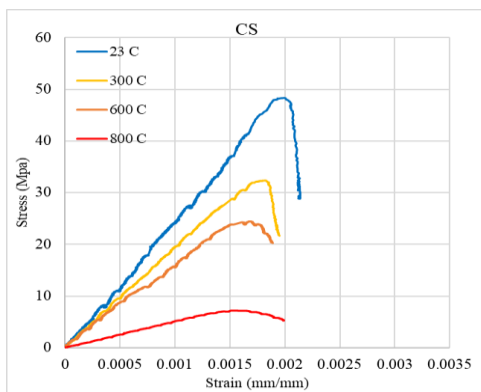
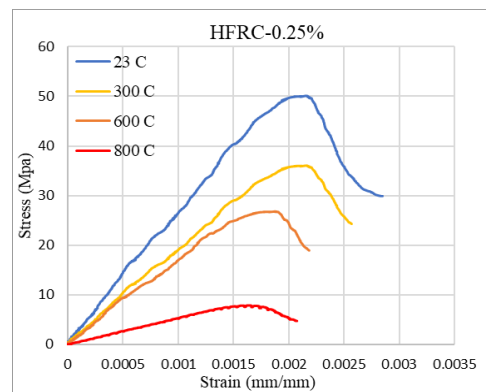


**Figure 13:** Fiber Crack Arresting Mechanism.

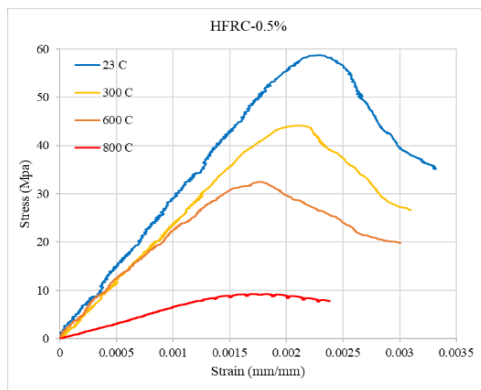
However, 0.5% of the modified samples performed better than any of the other modified formulations because, at temperatures of 300, 600, and 800<sup>o</sup>c, they maintained up to 75%, 55%, and 18% of their original strength.



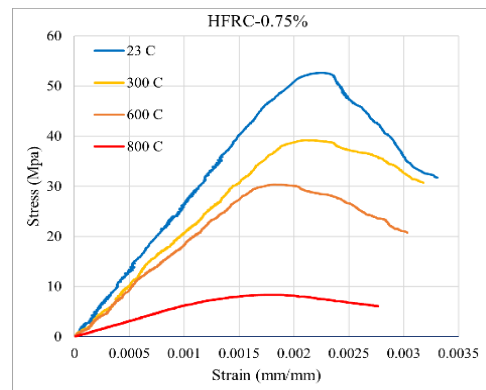
(a)



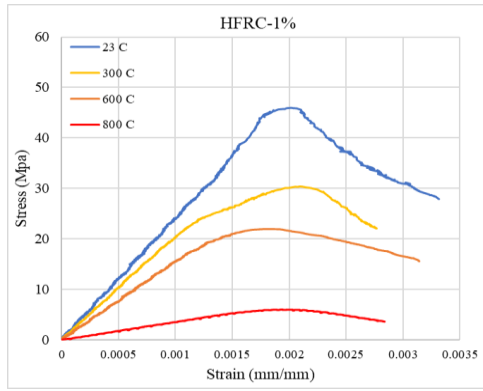
(b)



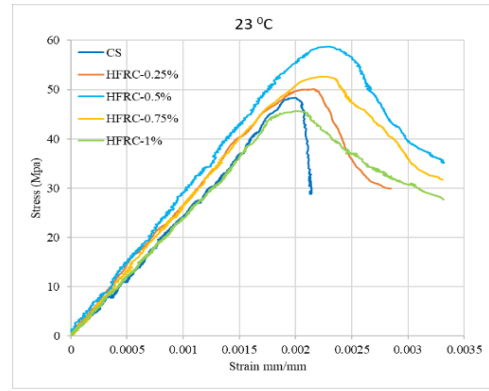
(c)



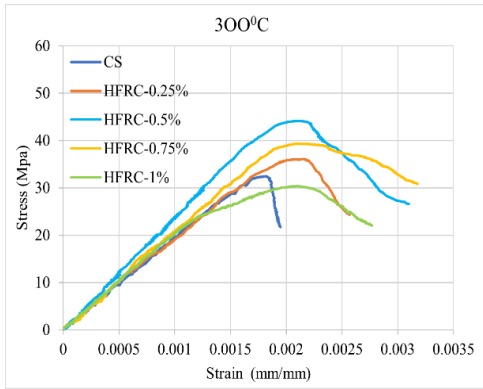
(d)



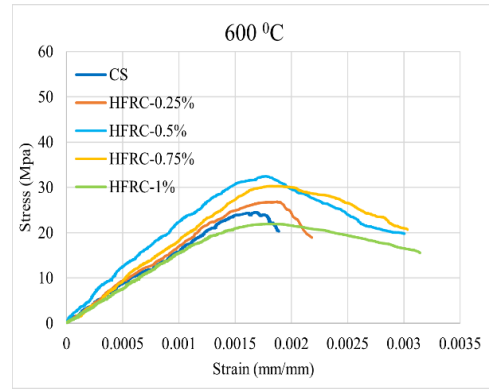
(e)



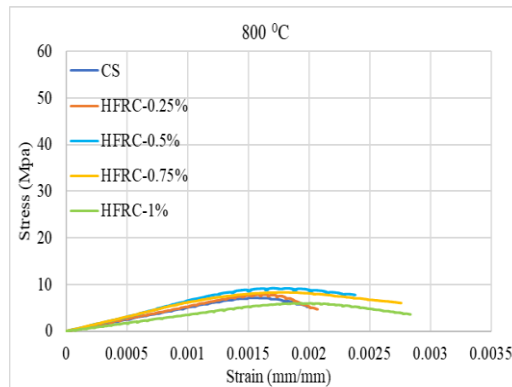
(f)



(g)



(h)



(k)

**Figure 14:** Stress-Strain Curve of Cylinders.

However, samples treated with 0.75% at 300, 600, and 800<sup>0</sup>c maintained up to 74.64%, 57.58%, and 16.58% of their initial values, respectively. The modifier samples having 0.25% HF at 300, 600 and 800 °C retained up to 71.54%, 53.26%, and 15.26% of their initial values. In addition, the increase in values compared to the control samples at the ambient level was approximately 4%, 22.56% and 9.56% for 0.25%, 0.5%, and 0.75% hybrid fibers additives respectively. Although, strength increases when HF content

increases to 0.75%, after this when fiber content increases to 1% then strength reduction occurs. At ambient level the strength of HFRC-1% is 4.05% less than control sample, at 300 °C, 600 °C, and 800°C it was 6.35%, 10.33% and 16.19%. However, the toughness, post crack energy increases with increasing fibers, which enhances ductility of concrete.

#### **4.2.3 Modulus of Elasticity E**

The modulus of elasticity as per ([ASTM C469/C469M-14 2014](#)) was derived from the stress-strain plots [88]. When temperature increases, then elastic modulus decreases, and it is dependent on several parameters, including aggregate type, w/c ratio, exposure temperatures, and microstructure. Decrease in elastic modulus of concrete with rise in temperature can be due to the transformation of cement hydrates, which causes a change in microstructure, a rise in shrinkage, and ultimately the chemically bound water loss produced by this reaction. Test outcome indicated that retention of modulus of elasticity of modified samples is higher than control sample especially in the range of 300-800°C, by crack bridging action of fibers reinforcement. The addition of fibers alters brittle behavior to elastic mode.

The mean elevation in modulus of elasticity at normal temperature of 0.25%-HFRC, 0.5%-HFRC, and 0.75%-HFRC is around 2.16%, 9.92 %, and 4.69% compared to CS, respectively, while decreased with 1%-HFRC by 2.14% than CS. The strain at the compressive strength is positively associated with fiber volumetric ratio. This showed that an increase in HF content led to an increased increase in the strain. On the other hand, the elastic modulus had a negative correlation, which suggests that a rise in the fiber volumetric ratio resulted in a drop in the elastic modulus. When the fiber content in concrete exceeded 0.75%, a little reduction in the elastic modulus of concrete was noted. The integration of increased amount of fiber may be responsible for the existence of extra voids in concrete [103]. The reduction in modulus of elasticity of 0%, 0.25%-HFRC, 0.5%-HFRC, 0.75%-HFRC and 1%-HFRC at 300°C are 17.87%, 12.77%, 13.6% and 18.7% respectively. At 600°C the reduction in E is 28.558%, 26.8%, 25.15%, 23.89, and 30.89%. Modulus of elasticity decreases sharply after 600°C, at 800°C the value of E reduced to 61.38%, 60.43%, 60.28%, 59.68% and 63.62% Correspondingly. The better performance of the modified samples may be associated with stabilizing the load-carrying area by means of greater interlocking and improved adhesion between the fibers and the cement matrix. The inclusion of steel fibers improves elastic modulus up to dose of 1% [45].

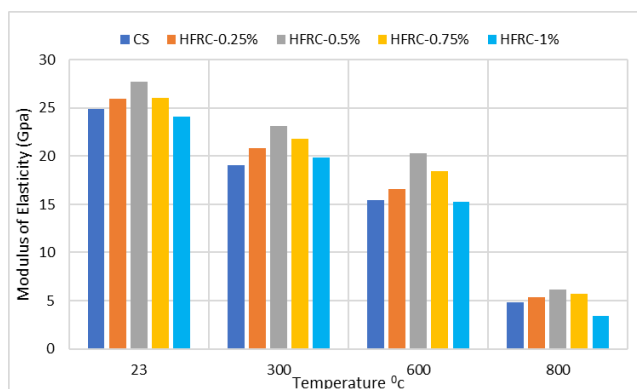


**Figure 15:** Modulus of Elasticity Of Concrete Cylinders.

#### 4.2.4 Compressive Failure Mode

After the application of the high-temperature treatment, the cylinders were put to compression testing (as seen in Fig. 19). The outcomes of these experiments demonstrated the causes of failure for a variety of concrete mixes, with each mix being a representative random pick from a set of three mixtures. As the load was applied to the control samples to their nearest maximum threshold, vertical cracks appeared on the concrete, having an audible cracking sound. Following the occurrence of peak load, the cracks exhibited rapid propagation throughout the specimen, resulting in a quick failure process. The experimental results obtained from the tests conducted on cylinders subjected to 600<sup>0</sup>c- 800<sup>0</sup>c revealed spalling off concrete cylinders at the maximum load for the control sample, while only cracks were observed for the HF modifier samples. When exposed to high temperatures, concrete cylinders that include HF do not completely deteriorate as quickly as those that do not have HF. When the quantity of HF in the mixture was higher, the cylinders produced after the compression test were more integral. When fibers content increases, the cracks follow a zigzag pattern. Lateral expansion was observed, especially with 1% HF modifier samples. The failure pattern of HFRC was quite ductile. After being subjected to a compression test, the cylinders' structural integrity is improved according to the quantity of HF in the material. At elevated temperature failure pattern of HFRC-0.5% and HFRC-0.75% is different from other additives and control sample. It is cleared from Fig 19 cracks in the control sample is vertical while in fibers additives the cracks pattern is zigzag.

23<sup>0</sup>c

300<sup>0</sup>c

600<sup>0</sup>c

800<sup>0</sup>c

CS



HFRC-  
0.25%



HFRC-  
0.5%



HFRC-  
0.75%

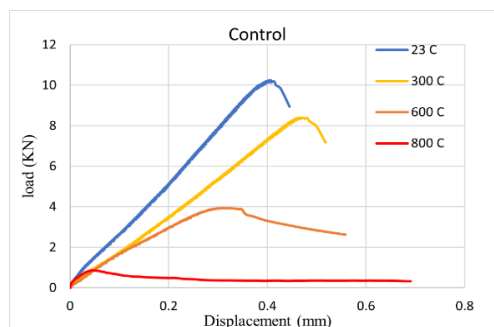




**Figure 16:** Compressive Failure Mode of Cylinders at Targeted Temperatures.

#### 4.2.5 Load Vs Displacement Variations

A load system designed for flexural testing; we were able to determine the ultimate load at which specimens collapsed when subjected to varying temperatures. Load versus displacement values that are dependent on temperature have been shown for hybrid fiber-reinforced specimens. The dimension of beam sample was [100x100x400 mm] based on [ASTM C293/C239M-16](#). In all the Figures 0.5% of the modified samples performed better in terms of load retention than any of the other modified formulations at 300<sup>0</sup>c ,600<sup>0</sup>c and 800<sup>0</sup>c it retained up to 82.26%, 38.96%, and 11.32% of their original values. While 0.75% modified samples at 300<sup>0</sup>c ,600<sup>0</sup>c and 800<sup>0</sup>c retained up to 90.28%, 42.21% and 13.11% of their strength at room temperature. In addition, 0.25% HF modifier samples at 300<sup>0</sup>c, 600<sup>0</sup>c and 800<sup>0</sup>c retained up to 81.42%, .34% and 12.22% of their original value. 1% additive retain up to 82.25%, 38.68%, and 13.01% while control sample retain up to 81.29%, 32.48% and 8.3% respectively, to their original value.



(a)

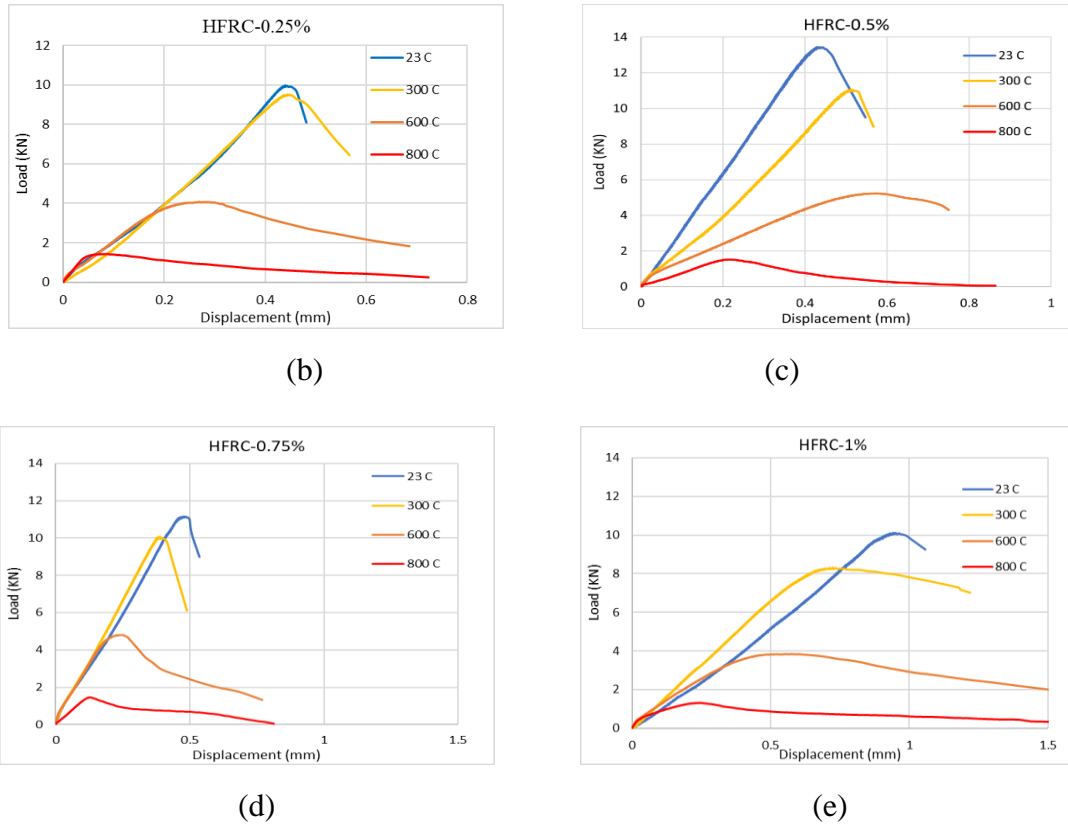


**Figure 17:** Load Vs Deflection Curve of Beams with Different Elevated Temperatures.

#### 4.2.6 Flexural Strength

Flexural strength is an indirect measure of the material's tensile strength, also called modulus of rupture, which is a material's ability to bend without breaking. When HF is added to concrete, there was a noted rise in bending strength. This can be attributed to HF's superior tensile properties, the strong bond between the fibers and the matrix facilitating force distribution, and the even distribution of fibers within the matrix. At higher temperatures, modified samples outperformed control samples in terms of performance and improved fire endurance due to force transfer mechanism from matrix to fibers. Steel fibers have a higher thermal conductivity, this property of steel fibers makes it easier for heat to flow inside concrete, which slows the growth of cracks. Consequently, specimens with steel fibers have increased flexural strength [44]. In addition, basalt fibers trap air inside concrete, which serves to dissipate heat and reduces the amount of integrity lost at high temperature [12]. It was examined that with increasing fibers content flexural strength was increased by 6-15% at normal temperature. Essentially, the joining effect of the equally spaced fibers across the fractures effectively inhibits the spread of small fissures in the initial phase and successfully delays the formation of large cracks at subsequent stages. As a result, the

flexural strength is increased. Temperature increase results in a reduction in flexural strength [104].

The remaining strength of concrete with 0.5% HF surpassed that of other samples at both standard and increased temperatures. However, strength degradation at 300<sup>0</sup>c, 600<sup>0</sup>c and 800<sup>0</sup>c of HFRC- 0.75% is lower than other additive and control sample. When compared to the Control specimens, the HFRC specimens show excellent increases in strength at ambient levels as modified 0.25%, 0.5%, and 0.75% specimens exhibit increases in strength by 6%, 15%, and 9%, respectively, as shown in Figure 21. The sample with 1% fibers had a 3% lower flexural strength than the CS sample, which might be due to an irregular scattering of the fibers, in addition to a weaker stickiness with the cement paste. Furthermore, fiber coagulation may result in excessive voids, resulting in a less dense matrix with lesser strength. The flexural strength degradation at 300<sup>0</sup>c of CS, HFRC-0.25%, HFRC-0.5%, HFRC-0.75%, and HFRC-1% was about 18.03%, 15.41%, 14.02%, 9.79% and 17.74% respectively. At 600<sup>0</sup>c the downfall of CS, HFRC-0.25%, HFRC-0.5%, HFRC-0.75%, and HFRC-1% was about 61.15%, 59.41%, 57.02%, 56.79% and 62.74%. Furthermore, at 800<sup>0</sup>c the residual strength of CS, HFRC-0.25%, HFRC-0.5%, HFRC-0.75%, and HFRC-1% was about 91.15%, 87.41%, 88.02%, 86.79% and 86.89% of their original strength respectively. Due to the reinforcing capabilities of fiber, using fiber in cement compounds results in a stronger link between the cement compounds and the aggregate. However, the decrease in bending strength that occurs at higher temperatures is caused by unequal expansion between the aggregate and cement layers as well as the production of extra internal stresses inside the concrete itself. Furthermore, increasing fiber content beyond optimum level may reduce cement which causing reduction in strength.

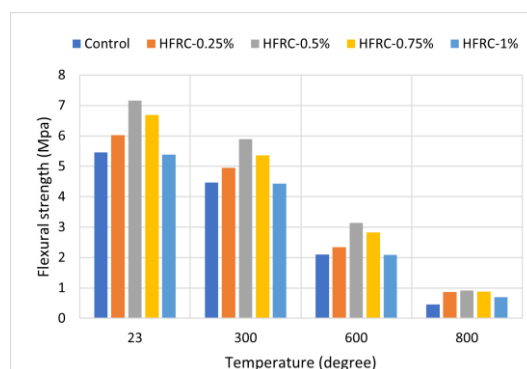


**Figure 18:** Flexural Strength of Beams with Different Temperatures.

#### 4.2.7 Energy Absorption Capacity (Toughness)

The compressive toughness (TC) of concrete is determined by calculating the area below the stress-strain curve until there is a decrease of 20% in the peak stress. This measurement determines how much energy the concrete can absorb before it breaks and how well it can resist deformation when compressed [105], [106]. When temperature increases, the compressive strength and peak strain of all samples decreases, which leads to a reduction in the material's toughness. At room temperature, it was discovered that the inclusion of steel fibers had a favorable impact on the toughness of FRC [107], [108]. Abrasion resistance and toughness may all be significantly improved in concrete by including even a tiny number of basalt fibers as a reinforcing element [109]. When compared to PC, steel fibers almost doubled the toughness of unheated concrete, and this capacity also increased when the concrete was heated to higher temperatures [75]. If the specimen has a larger compression energy, this suggests that the matrix is performing more effectively.

The Energy absorption values for each specimen (CS, HFRC-0.25%, HFRC-0.5%, HFRC-0.75%, and HFRC-1%) were determined and charted against specific temperatures as shown in Fig 22. At room temperature, data indicated HSC total energy intake is 0.1757 which is lesser than 0.22566, 0.276739, 0.282578 and 0.235951, for HFRC-0.25%, HFRC-0.5%, HFRC-0.75%, and HFRC-1%), respectively. The results demonstrate that introducing hybrid fibers increases energy absorption while decreasing with escalating temperature. It was observed at ambient temperature, 300<sup>0</sup>c and 800<sup>0</sup>c toughness of modified samples increases up to HFRC-0.75%, further increases in fiber content decreases in toughness, which can be attributed to creation of voids and lower adhesion of fibers with cement at higher dosage.

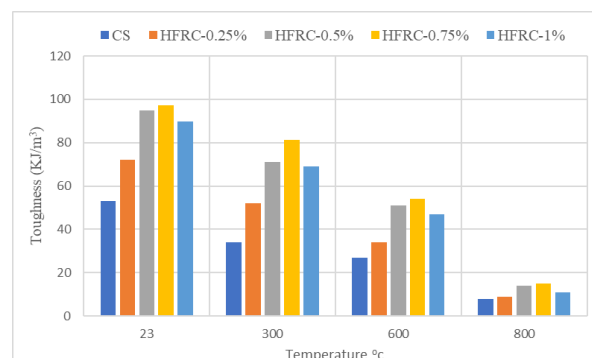


**Figure 19:** Compressive Toughness of Concrete Cylinders at Different Temperatures.

#### 4.2.8 Compressive Toughness Index

The toughness index (TI) is a representation of the percentage of change, whether that change is an increase or a reduction, in the sample of modified hybrid fibers in comparison to the control sample material at the given temperatures.

$$TI = \frac{T_c \text{ of fibers modified concrete samples at the targeted temperature}}{T_c \text{ of control samples at the target temperature}} \quad [110].$$

The compressive toughness index of all samples is shown in Fig 23. The decrease or increase in toughness index of modified sample can be defined from the baseline of control sample. The toughness index at 23<sup>0</sup>c, 300<sup>0</sup>c, and 800<sup>0</sup>c for the modified sample increases to 0.75% fiber additive, and a further increase in fiber content decreases. However, TI of 1% additive is still higher than control sample. TI of modified samples i.e., HFRC-0.25%, HFRC-0.5%, HFRC-0.75%, and HFRC-1%, at ambient temperature was 28.95%, 57.69%, 60.49%, and 34.26% relative to the control specimens. TI is a useful tool for accurately measuring the increased energy consumption in the modified specimens [101]. When compared to the control specimen, modified samples demonstrate a similar pattern of rising toughness index with increases of 29.63%, 64.4%, 85.92%, and 81.13%, respectively, at 300<sup>0</sup>c. The increasing trend in toughness index of modified samples at 600<sup>0</sup>c and 800<sup>0</sup>c up to 28.3%, 55.10%, 77.97%, 85.79% and 25.29%, 94.41%, 85.55%, 52.24% respectively. This toughness index behavior suggests that the hybrid fibers in the sample matrix have improved deformability and fracture resilience. Toughness index indicates towards enhanced fracture and ductility characteristics [105]. The area that lies under the stress-strain curve is used in the calculation of the toughness index (TI). This area displays how much energy the specimen can absorb before it fails and predicts how well the specimen can withstand deformation when subjected to compression.

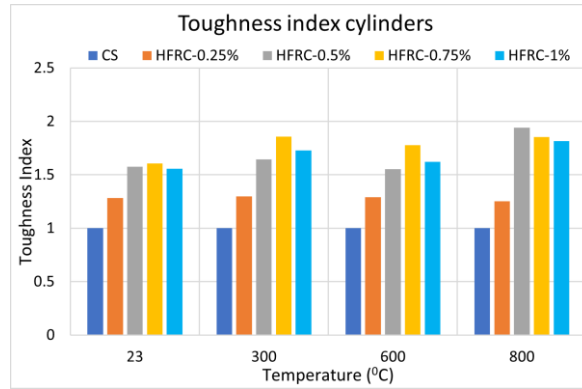


**Figure 20:** Compressive Toughness Index is a Function of Temperature.

#### 4.2.9 Crack Energy and Toughness Index

The area under the load-deflection curve from zero to ultimate load is used to calculate total absorbed energy, also known as flexural toughness; this value cannot exceed 20% of the material's peak strength [ASTMC 1609](#) [112]. The higher the fiber content, the greater the resistance to the propagation of cracks, and less steep the load-deflection curve of the HFRC beyond the peak load. The crack energy and ductility of concrete is enhanced by bridging effect of HF, thus sudden failure after peak load is eliminated. It was determined from the results that HFRC has a slower load drop after peak and superior load absorption capacity than CS [100]. The hybrid fibers increased ductility and crack energy, preventing brittle failure after maximum load due to the bridge effect. It was observed at ambient temperature that total energy absorb for CS is 2.54 KN.mm which is lower than 2.64 KN.mm, 4.35 KN.mm, 4.561 KN.mm and 3.921 KN.mm for HFRC-0.25%, HFRC-0.5%, HFRC-0.75% and HFRC-1% respectively. There is an increase in energy absorption by adding HF at all target temperatures. In [Fig 24](#) it was observed at all temperatures, toughness increases up to 0.75%, further increases in fiber content decreases in crack energy.

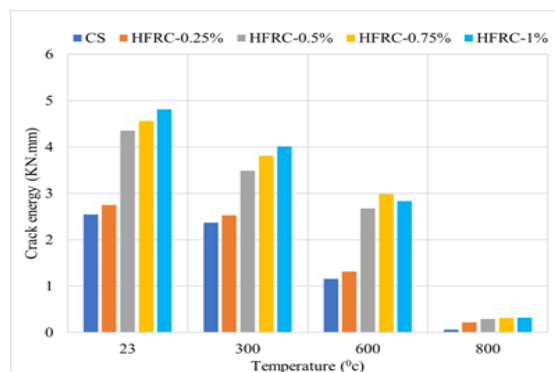


**Figure 21:** Crack Energy is a Function of Temperature.

The HFRC enhanced resistance against load as compared to CS due to the addition of HF. Opposition to load is due to load transferring mechanism from concrete to hybrid fibers. The decline trend is observed with 1% additive at 600<sup>0</sup>c. If the specimen has a larger crack energy this suggests that the matrix is performing more effectively. However, crack energy decreases with escalating temperature due to decreased HFRC and the control sample strength. The crack energy at 300<sup>0</sup>c, 600<sup>0</sup>c of 0%, HFRC-0.25%, HFRC-0.5%, HFRC-0.75%, and HFRC-1% decreases by 6.6%, 4.54%, 19.77%, 16.64%, 17.113% and 54.72%, 50.37%, 33.56%, 34.66%, 27.82% respectively. The decreasing trend of crack energy was very quick for 800<sup>0</sup>c which is 97.63%, 92.04%, 93.33%, 93.32%, 95.16% respectively.

The composite has a greater proportion of steel with a high elastic modulus and tensile strength, it can absorb more energy after the first fracture. The kind of fiber, its length, and the amount of fiber used are the three most important parameters that determine the toughness index. The toughness index defines quality of fiber and discriminates b/w low and high-energy absorbing fiber and mix. The toughness index of modified sample is greater than control sample observed at all temperatures.

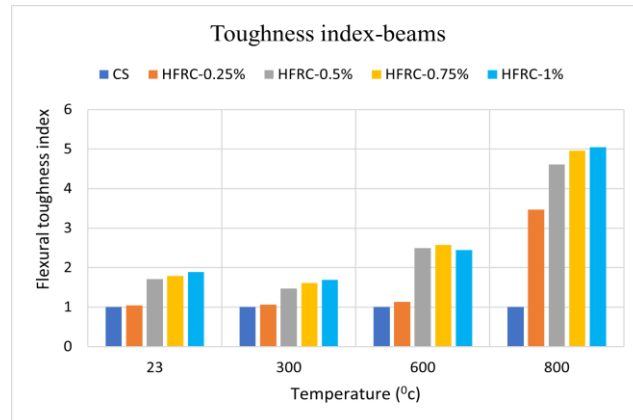


**Figure 22:** Flexural Toughness Index is a Function of Temperature.

In Fig 25 it is cleared at ambient temperature that incremental increases in toughness index of modified sample as compared to control samples was 4%, 71%, 79% and 54% respectively. At temperature of 300<sup>0</sup>c and 600<sup>0</sup>c a similar improvement in toughness index of modified sample was observed with an increase of 2%, 13% 10%, 11% and 9%, 45%, 43%, 58%, respectively compared to control sample. The toughness index behavior implies that the hybrid fibers in the sample matrix have improved deformability and fracture resilience.

#### 4.2.10 Mass Loss

Concrete exposed to elevated temperature, the evaporation of freely present moisture within the concrete's pores and chemically bound water because of conversion reaction take place leading to mass loss [113]. The ratio of mass at target temperature to mass at ambient temperature ( $M_t/M$ ) was determined to assess the amount of mass loss that occurred across all the samples [105]. It was observed from previous studies that change in mass at elevated temperature conditions is contingent upon the type of hydration products and aggregates utilized in the construction of the concrete [114]. High strength concrete modifier shows minute mass loss in range of 300<sup>0</sup>c to 800<sup>0</sup>c than control sample. Under extreme heat conditions up to 800<sup>0</sup>c. The reduced mass in altered sample is traced back to the elevated presence of nucleation site. This phenomenon is inherent in basalt, which nucleates at rising temperature [35]. The primary element influencing the thermal stability of basalt fibers is their behavior in terms of crystallization. Essentially, the high levels of iron oxides in basalt fiber play a key role in initiating the crystallization process. The burning of ferrous cations marks the beginning of this process, which ultimately leads to the creation of a spinel-like structural stage on the surface of the fiber. Divalent cations such as calcium, magnesium, and iron diffuse from the core of the fiber to its surface, where they chemically combine with oxygen in the surrounding to produce nanocrystalline layers of CaO, MgO, and (Mg, Fe)<sub>3</sub>O<sub>4</sub>. Furthermore, as the temperature increases, the nucleation sites formed by the spinel crystals facilitate the crystallization of pyroxene phases [26]. Apart from the basalt fibers steel fibers also perform thermally stability at elevated temperature, because of high density and was confirmed by [114].

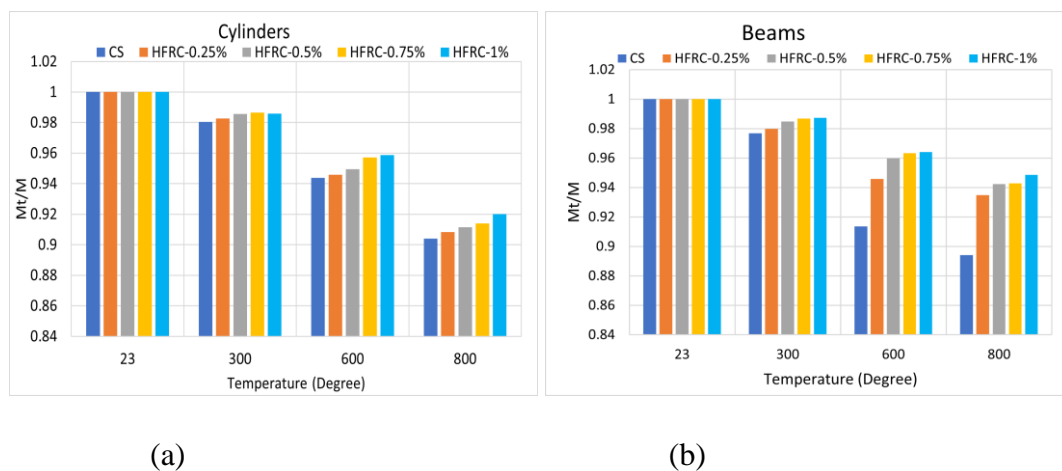
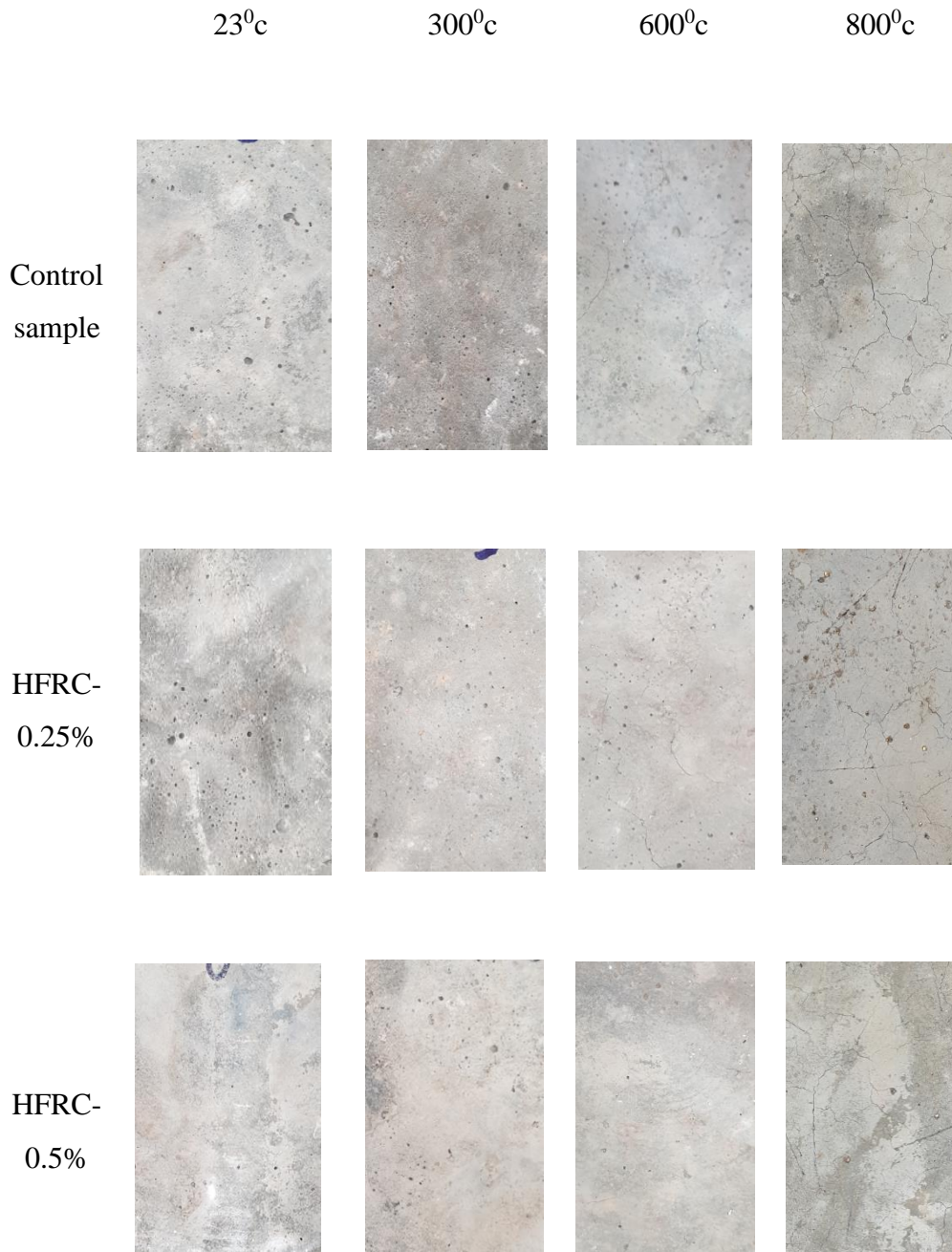


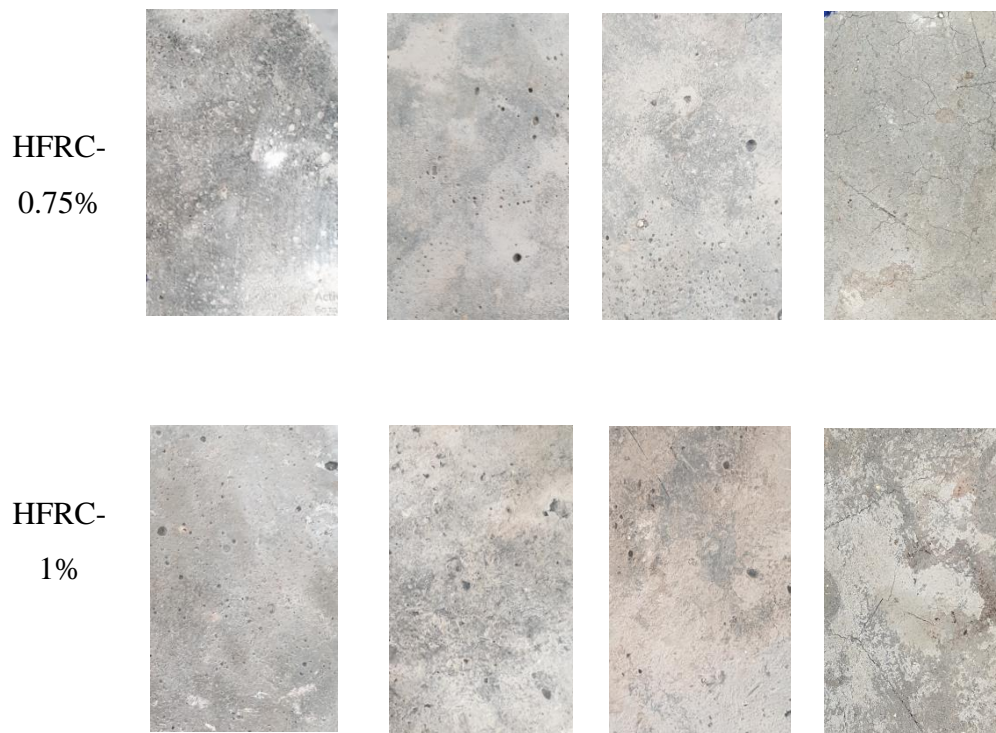
**Figure 23:** Mass Loss of Concrete Cylinders with Varying Temperature, (b) Mass Loss of Concrete Beams with Varying Temperature.

#### 4.2.11 Visual Inspection

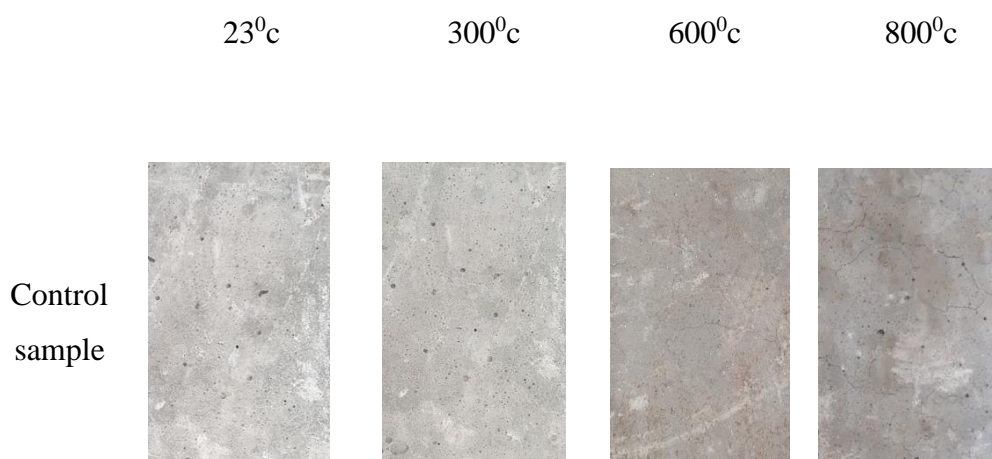
The ability to evaluate the serviceability of fire damage concrete depends on visual observation. The emergence of cracks and alterations in color can provide comprehensive insights regarding the temperatures to which the material was exposed [110]. Thoroughly assessing the fire-damaged structure is essential, involving comprehensive examination to conclude the severity of fire, which includes visible deterioration, the scale of the fire, and the pattern of its spread [5]. Elevated temperatures primarily induce thermal cracking and crazing in concrete by vaporization, dehydration of the binding paste, and breakdown of the microstructure [113]. A visual analysis of both control and altered high-strength concrete (HSC) exposed to temperatures ranging from 23-800<sup>0</sup>c reveals localized cracking, as displayed in [Fig 27 and 28](#). The pattern of fissures was consistent, and less cracking was noticeable in the modified samples in comparison to the CS within the 600-800<sup>0</sup>c range. There was no significant surface cracking detected on any of the samples when subjected to temperatures ranging from 23 to 300 degrees Celsius. This may be attributed to a less significant weakening of the aggregate-paste bond as well as a reduced thermal gradient between the specimen's core and surface. A considerable number of visible cracks were observed at 600<sup>0</sup>c in control and 0.25% hybrid modifier concrete, however minor cracks were found on 0.5% and 0.75% additives while fewer hair line cracks on surface of 1% additive HFRC. At 800<sup>0</sup>c severe cracks were observed in control and modifier except 1% additive, where cracks were less as compared to others. The modified samples demonstrated a higher resistance to cracking, because of the effective role of hybrid fibers within the concrete matrix in countering tensile thermal stresses. Cracking in modifier specimen was observed to be less compared to control sample. However, at elevated temperature the presence of partially or fully melted basalt fibers resulted in the creation of channels on the fiber bed. These channels acted as passageways for the vapor and gases that were being produced within the specimen, allowing them to escape. These interconnected channels within the specimen facilitated the exit of gases and vapors, thereby reducing the buildup of internal pressure and minimizing the occurrence of cracks [12]. The cracking is initially, can be attributed to the thermal expansion of cement paste, which results in localized ruptures in the connection between cement and aggregate. At elevated temperatures, the drying shrinkage, driven by water loss, begins to surpass thermal expansion. These two contrasting mechanisms gradually

deteriorate and fracture the concrete. In Steel fiber reinforced concrete lesser cracks were observed, which showed that Presence of steel fibers can delay cracks by bridging effect [50]. Visual observation of concrete samples revealed no significant color change until 600<sup>0</sup>c.





**Figure 24:** External Surface of Concrete Cylinders at Different Temperature.



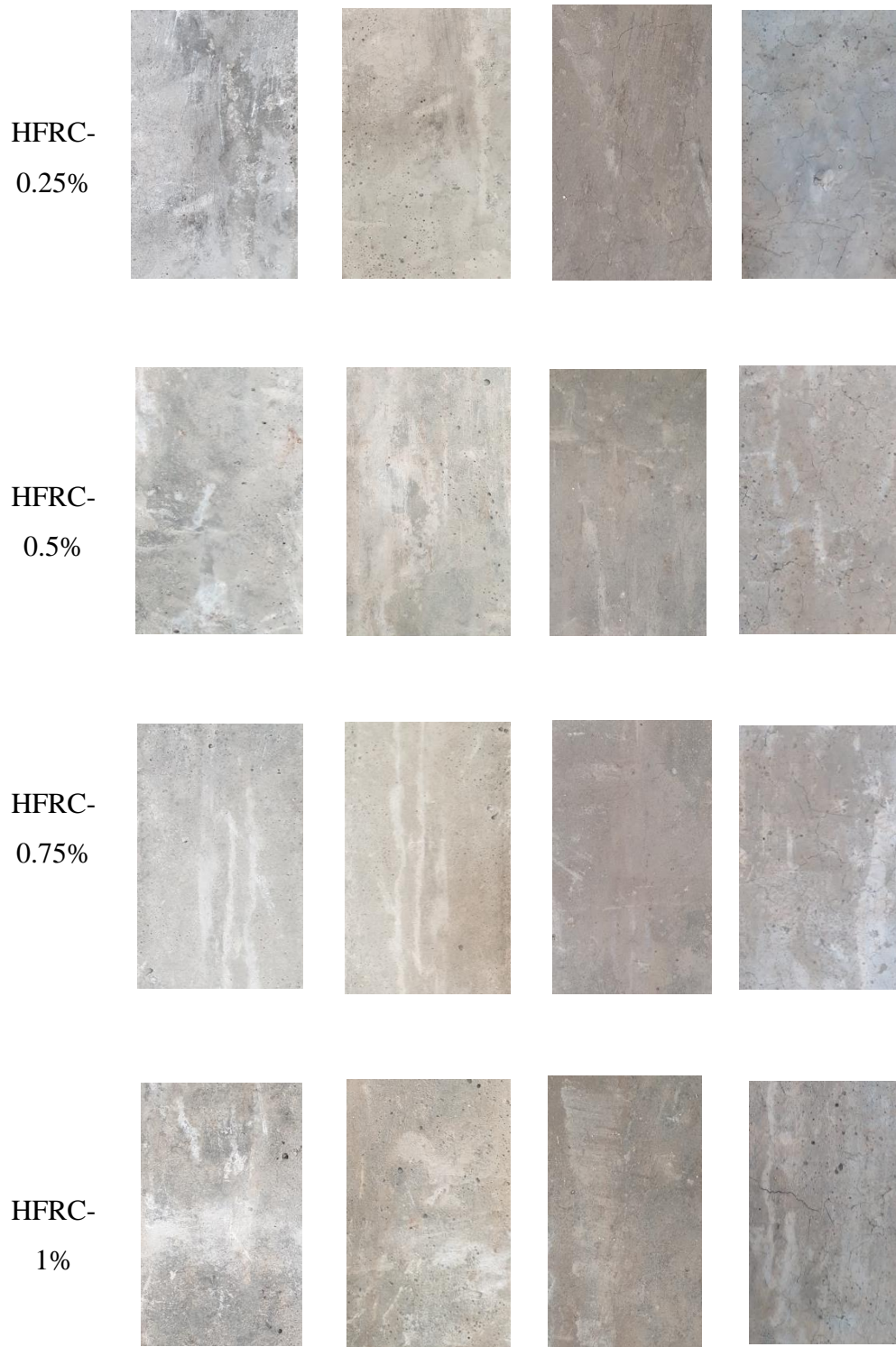


**Figure 25:** External Surface of Concrete Beams at Different Temperature.

## CHAPTER 5

### CONCLUSION AND RECOMMENDATION

#### 5.1 Conclusion

Based on the facts presented, the following are the findings drawn from this empirical study.

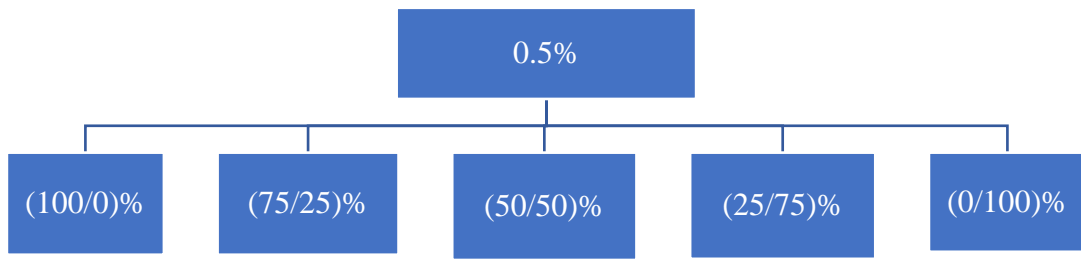
- The incorporation of hybrid fiber results in a significant improvement in the mechanical characteristics of concrete, which can be seen prior to as well as after exposure to fire. However, the degree of strength enhancement is contingent upon the quantity of fibers, the composition of the mix, and the dispersal of fibers within the concrete. Nevertheless, superior endurance in terms of maintaining strength and structural integrity is noticeable at elevated temperatures by HFRC.
- The compressive strength enhancement at ambient temperature was 4.39%, 22.41% and 9.61% for (HFRC-0.25%, HFRC-0.5% and HFRC-0.75%) respectively as compared to CS, in addition to 1% HFRC decreases strength to 4.25% from control sample. At 600°C, control sample, 0.25%, 0.5%, 0.75%, and 1% additives retain their strength up to 50%, 53.57%, 55.28%, 57.12% and 52.23% respectively. While at 800°C, specimens retained up to 14.49%, 15.69%, 16.12%, 16.25% and 13.05% of their original strength, respectively.
- The incorporation of HF to the concrete mix increased the flexural strength by 6%, 15.12% and 9% for HFRC-0.25%, HFRC-0.5% and HFRC-0.75%, respectively as compared to control sample, considering HFRC-1% the flexural strength reduced to 3% as compared to CS. At 800°C control sample, 0.25%, 0.5%, 0.75%, and 1% additives retained about 8.39%, 14.38%, 12.76%, 13.11% and 13.05% of their original flexural strength, respectively.
- The decrease in strength is related to mix heterogeneity induced by higher hybrid fiber content, which also lowers amount of cement. In addition, non-uniform distribution and cluster of fibers causing internal voids decreasing strength. Moreover, the crack connecting effect, high tensile strength of hybrid fiber and filler effect of basalt fiber results in improved properties.
- After being subjected to compression testing, cylinders with a higher percentage of hybrid fibers retain a higher level of integrity. Moreover, when the percentage

of fibers in the material increases, fractures will often become more zigzag-shaped and spread.

- A rise in the amount of HF in concrete enhances both ultimate and peak strain because HF contributes to crack resistance after the peak load is reached. The improved strain capacity at ambient and elevated temperature indicates the beneficial impact of HF compared to the reference sample.
- The existence of HF in the mix leads to gradual decline in the mechanical characteristics of HFRC as temperature rises, owing to reinforcing action and better fire resistance, compared to the control sample, apart from mix containing 1% additives.
- The weight reduction of concrete for HFRC was relatively less compared to control sample. It is due to the nucleation site of basalt fiber at high temperature and substantial density of steel fiber.
- The inclusion of Hybrid fibers prevented crack growth through fiber bridging, resulting in delayed crack propagation and significant enhancement in the toughness of HFRC. The optimum content of hybrid fibers to achieve high toughness was found to be 0.75% and 1% additives.
- The stress-strain curve of modified concrete exhibits a notable difference as compared to control sample and increases with increasing fibers content.
- Surface cracking from visual assessment in modifier specimen was observed to be less compared to control sample. However, at elevated temperature the presence of partially or fully melted basalt fibers resulted in the creation of channels on the fiber bed. These channels served as conduits allowing the internally produced vapors and gases from the sample to be released, which reduced the buildup of internal pressure and minimizing the occurrence of cracks. The bridging effect of steel fibers also contributes to reducing cracks.

## **5.2 Recommendations**

- Further study can be done on 0.5% HF in concrete under compression and flexural for ambient as well as on elevated temperature. What's the best ratio between steel and basalt fibers to withstand high temperatures? Is it a 1:1 ratio, or does one fiber dominate? in concrete under compression test for ambient as well as on elevated temperature? Apart from this impact resistance, durability, ductility, and chemical resistance can also be studied.



## REFERENCES

- [1] W. Khaliq and V. Kodur, "Behavior of high strength fly ash concrete columns under fire conditions," *Materials and Structures/Materiaux et Constructions*, vol. 46, no. 5, pp. 857–867, May 2013, doi: 10.1617/s11527-012-9938-7.
- [2] Q. Ma, R. Guo, Z. Zhao, Z. Lin, and K. He, "Mechanical properties of concrete at high temperature-A review," *Construction and Building Materials*, vol. 93. Elsevier Ltd, pp. 371–383, Jun. 16, 2015. doi: 10.1016/j.conbuildmat.2015.05.131.
- [3] R. Khan, S. H. Farooq, and M. Usman, "Blast loading response of reinforced concrete panels externally reinforced with steel strips," *Infrastructures (Basel)*, vol. 4, no. 3, Aug. 2019, doi: 10.3390/infrastructures4030054.
- [4] Z. Huang, J. Y. R. Liew, and W. Li, "Evaluation of compressive behavior of ultra-lightweight cement composite after elevated temperature exposure," *Constr Build Mater*, vol. 148, pp. 579–589, Sep. 2017, doi: 10.1016/j.conbuildmat.2017.04.121.
- [5] A. Aseem, W. Latif Baloch, R. A. Khushnood, and A. Mushtaq, "Structural health assessment of fire damaged building using non-destructive testing and micro-graphical forensic analysis: A case study," *Case Studies in Construction Materials*, vol. 11, Dec. 2019, doi: 10.1016/j.cscm.2019.e00258.
- [6] P. R. Vardhan and T. M. Rao, "Elevated Temperature and Durability Studies on High Strength Concrete", doi: 10.32377/cvrjst1502.
- [7] M. R. Bangi and T. Horiguchi, "Pore pressure development in hybrid fibre-reinforced high strength concrete at elevated temperatures," *Cem Concr Res*, vol. 41, no. 11, pp. 1150–1156, 2011, doi: 10.1016/j.cemconres.2011.07.001.
- [8] A. Behnood and M. Ghandehari, "Comparison of compressive and splitting tensile strength of high-strength concrete with and without polypropylene fibers heated to high temperatures," *Fire Saf J*, vol. 44, no. 8, pp. 1015–1022, 2009, doi: 10.1016/j.firesaf.2009.07.001.
- [9] S. L. E. O. Suhaendi and T. Horiguchi, "Fiber-reinforced High-strength Concrete under Elevated Temperature — Effect of Fibers on Residual Properties," pp. 271–278, 2005.
- [10] R. Kodur, "Fire Performance of High-Strength Concrete Structural Members," pp. 1–4.
- [11] J. R. Lawson and L. T. Phan, "NISTIR 6475 Mechanical Properties of High Performance Concrete After Exposure to Elevated Temperatures NISTIR 6475 Mechanical Properties of High Performance Concrete After Exposure to Elevated Temperatures".
- [12] A. Alaskar, A. Albidah, A. S. Alqarni, R. Alyousef, and H. Mohammad hosseini, "Performance evaluation of high-strength concrete reinforced with basalt fibers exposed to elevated temperatures," *Journal of Building Engineering*, vol. 35, Mar. 2021, doi: 10.1016/j.job.2020.102108.
- [13] L. T. Phan and N. J. Carino, "Code provisions for high strength concrete strength-temperature relationship at elevated temperatures," vol. 36, no. March, pp. 91–98, 2003.

- [14] V. Kodur and S. Banerji, "Modeling the fire-induced spalling in concrete structures incorporating hydro-thermo-mechanical stresses," *Cem Concr Compos*, vol. 117, Mar. 2021, doi: 10.1016/j.cemconcomp.2020.103902.
- [15] H. Wu, X. Lin, and A. Zhou, "A review of mechanical properties of fibre reinforced concrete at elevated temperatures," *Cem Concr Res*, vol. 135, no. April, p. 106117, 2020, doi: 10.1016/j.cemconres.2020.106117.
- [16] Z. Yuan and Y. Jia, "Mechanical properties and microstructure of glass fiber and polypropylene fiber reinforced concrete: An experimental study," *Constr Build Mater*, vol. 266, Jan. 2021, doi: 10.1016/j.conbuildmat.2020.121048.
- [17] W. Yao, J. Li, and K. Wu, "Mechanical properties of hybrid fiber-reinforced concrete at low fiber volume fraction," *Cem Concr Res*, vol. 33, no. 1, pp. 27–30, Jan. 2003, doi: 10.1016/S0008-8846(02)00913-4.
- [18] K. F. Li *et al.*, "Effects of hybrid fibers on workability, mechanical, and time-dependent properties of high strength fiber-reinforced self-consolidating concrete," *Constr Build Mater*, vol. 277, Mar. 2021, doi: 10.1016/j.conbuildmat.2021.122325.
- [19] A. M. Zeyad, A. H. Khan, and B. A. Tayeh, "Durability and strength characteristics of high-strength concrete incorporated with volcanic pumice powder and polypropylene fibers," *Journal of Materials Research and Technology*, vol. 9, no. 1, pp. 806–813, Jan. 2020, doi: 10.1016/j.jmrt.2019.11.021.
- [20] S. T. Kang, J. Il Choi, K. T. Koh, K. S. Lee, and B. Y. Lee, "Hybrid effects of steel fiber and microfiber on the tensile behavior of ultra-high performance concrete," *Compos Struct*, vol. 145, pp. 37–42, Jun. 2016, doi: 10.1016/j.compstruct.2016.02.075.
- [21] D. Y. Yoo and N. Banthia, "Impact resistance of fiber-reinforced concrete – A review," *Cem Concr Compos*, vol. 104, Nov. 2019, doi: 10.1016/j.cemconcomp.2019.103389.
- [22] Y. Farnam, S. Mohammadi, and M. Shekarchi, "Experimental and numerical investigations of low velocity impact behavior of high-performance fiber-reinforced cement based composite," *Int J Impact Eng*, vol. 37, no. 2, pp. 220–229, 2010, doi: 10.1016/j.ijimpeng.2009.08.006.
- [23] H. S. Jr, S. F. Santos, M. Radonjic, and W. O. Soboyejo, "Cement & Concrete Composites Fracture and fatigue of natural fiber-reinforced cementitious composites," *Cem Concr Compos*, vol. 31, no. 4, pp. 232–243, 2009, doi: 10.1016/j.cemconcomp.2009.02.006.
- [24] Y. Li, K. H. Tan, and E. H. Yang, "Synergistic effects of hybrid polypropylene and steel fibers on explosive spalling prevention of ultra-high performance concrete at elevated temperature," *Cem Concr Compos*, vol. 96, pp. 174–181, Feb. 2019, doi: 10.1016/j.cemconcomp.2018.11.009.
- [25] P. Zhang, L. Kang, J. Wang, J. Guo, S. Hu, and Y. Ling, "Mechanical properties and explosive spalling behavior of steel-fiber-reinforced concrete exposed to high temperature-A review," *Applied Sciences (Switzerland)*, vol. 10, no. 7. MDPI AG, Apr. 01, 2020. doi: 10.3390/app10072324.
- [26] V. Fiore, T. Scalici, G. Di Bella, and A. Valenza, "A review on basalt fibre and its composites," vol. 74, pp. 74–94, 2015, doi: 10.1016/j.compositesb.2014.12.034.

- [27] Y. Yang, Q. Zhou, X. Li, G. C. Lum, and Y. Deng, "Uniaxial compression mechanical property and fracture behavior of hybrid inorganic short mineral fibers reinforced cement-based material," *Cem Concr Compos*, vol. 104, Nov. 2019, doi: 10.1016/j.cemconcomp.2019.103338.
- [28] S. K. Mezzal, Z. Al-Azzawi, and K. B. Najim, "Effect of discarded steel fibers on impact resistance, flexural toughness and fracture energy of high-strength self-compacting concrete exposed to elevated temperatures," *Fire Saf J*, vol. 121, May 2021, doi: 10.1016/j.firesaf.2020.103271.
- [29] M. A. Abd El-baky, M. A. Attia, M. M. Abdelhaleem, and M. A. Hassan, "Mechanical characterization of hybrid composites based on flax, basalt and glass fibers," *J Compos Mater*, vol. 54, no. 27, pp. 4185–4205, Nov. 2020, doi: 10.1177/0021998320928509.
- [30] M. Elsayed, F. Althoey, B. A. Tayeh, N. Ahmed, and A. A. El-Azim, "Behavior of eccentrically loaded hybrid fiber-reinforced high strength concrete columns exposed to elevated temperature," *Journal of Materials Research and Technology*, vol. 19, pp. 1003–1020, Jul. 2022, doi: 10.1016/j.jmrt.2022.05.079.
- [31] O. Düğenci, T. Haktanir, and F. Altun, "Experimental research for the effect of high temperature on the mechanical properties of steel fiber-reinforced concrete," *Constr Build Mater*, vol. 75, pp. 82–88, 2015, doi: 10.1016/j.conbuildmat.2014.11.005.
- [32] S. N. R. Shah, F. W. Akashah, and P. Shafiq, "Performance of High Strength Concrete Subjected to Elevated Temperatures: A Review," *Fire Technol*, vol. 55, no. 5, pp. 1571–1597, 2019, doi: 10.1007/s10694-018-0791-2.
- [33] J. Rubnerov, "Influence of thermal treatment on tensile failure of basalt fibers c i," vol. 69, pp. 1025–1033, 2002.
- [34] M. Science, "Chemical Durability and Mechanical Properties," vol. 27, no. 4, 2016, doi: 10.1177/0731684407084119.
- [35] J. Sim, C. Park, and D. Y. Moon, "Characteristics of basalt fiber as a strengthening material for concrete structures," vol. 36, pp. 504–512, 2005, doi: 10.1016/j.compositesb.2005.02.002.
- [36] C. Jiang, K. Fan, F. Wu, and D. Chen, "Experimental study on the mechanical properties and microstructure of chopped basalt fibre reinforced concrete," vol. 58, pp. 187–193, 2014.
- [37] X. E. Li, "Study on thermal resistance of basalt filament yarn," in *Advanced Materials Research*, Trans Tech Publ, 2011, pp. 666–669.
- [38] J. Branston, S. Das, S. Y. Kenno, and C. Taylor, "Mechanical behaviour of basalt fibre reinforced concrete," vol. 124, pp. 878–886, 2016.
- [39] T. M. Borhan, "Properties of glass concrete reinforced with short basalt fibre," vol. 42, pp. 265–271, 2012.
- [40] T. Ayub, N. Shafiq, and M. F. Nuruddin, "Effect of Chopped Basalt Fibers on the Mechanical Properties and Microstructure of High Performance Fiber Reinforced Concrete," vol. 2014, 2014.

- [41] X. Chaopeng and M. Ali, "Experimental and analytical study of hybrid fiber reinforced concrete prepared with basalt fiber under high temperature," no. December 2020, pp. 205–226, 2022, doi: 10.1002/fam.2968.
- [42] P. Zhang, L. Kang, J. Wang, J. Guo, S. Hu, and Y. Ling, "applied sciences Mechanical Properties and Explosive Spalling Behavior of Steel-Fiber-Reinforced Concrete Exposed to High Temperature — A Review," 2020.
- [43] R. Serrano, A. Cobo, M. I. Prieto, and M. de las N. González, "Analysis of fire resistance of concrete with polypropylene or steel fibers," *Constr Build Mater*, vol. 122, pp. 302–309, 2016, doi: 10.1016/j.conbuildmat.2016.06.055.
- [44] M. A. Moghadam, D. Ph, R. A. Izadifard, and D. Ph, "Effects of steel and glass fibers on mechanical and durability properties of concrete exposed to high temperatures," vol. 113, no. January, 2020.
- [45] G. M. Chen, Y. H. He, H. Yang, J. F. Chen, and Y. C. Guo, "Compressive behavior of steel fiber reinforced recycled aggregate concrete after exposure to elevated temperatures," *Constr Build Mater*, vol. 71, pp. 1–15, 2014, doi: 10.1016/j.conbuildmat.2014.08.012.
- [46] J. Xie, Z. Zhang, Z. Lu, and M. Sun, "Coupling effects of silica fume and steel-fiber on the compressive behaviour of recycled aggregate concrete after exposure to elevated temperature," *Constr Build Mater*, vol. 184, pp. 752–764, 2018, doi: 10.1016/j.conbuildmat.2018.07.035.
- [47] H. Wu, X. Lin, and A. Zhou, "A review of mechanical properties of fibre reinforced concrete at elevated temperatures," *Cem Concr Res*, vol. 135, no. April, p. 106117, 2020, doi: 10.1016/j.cemconres.2020.106117.
- [48] L. Yang, X. Lin, and R. J. Gravina, "Evaluation of dynamic increase factor models for steel fibre reinforced concrete," *Constr Build Mater*, vol. 190, pp. 632–644, 2018, doi: 10.1016/j.conbuildmat.2018.09.085.
- [49] O. Düğenci, T. Haktanir, and F. Altun, "Experimental research for the effect of high temperature on the mechanical properties of steel fiber-reinforced concrete," *Constr Build Mater*, vol. 75, pp. 82–88, 2015, doi: 10.1016/j.conbuildmat.2014.11.005.
- [50] A. Lau and M. Anson, "Effect of high temperatures on high performance steel fibre reinforced concrete," vol. 36, pp. 1698–1707, 2006, doi: 10.1016/j.cemconres.2006.03.024.
- [51] A. C. Institute, "State of the art report on high-strength concrete," *American Concrete Institute, Farmington Hills, Michigan*, 1992.
- [52] V. Kodur and R. Mcgrath, "Fire Endurance of High Strength Concrete Columns \*," pp. 73–87, 2003.
- [53] M. Mazloom, A. A. Ramezani-pour, and J. J. Brooks, "Effect of silica fume on mechanical properties of high-strength concrete," *Cem Concr Compos*, vol. 26, no. 4, pp. 347–357, 2004, doi: 10.1016/S0958-9465(03)00017-9.
- [54] J. M. Aldred *et al.*, "Guide for the use of silica fume in concrete," *ACI–American Concrete Institute–Committee: Farmington Hills, MI, USA*, vol. 234, p. 63, 2006.

- [55] M. I. Khan and R. Siddique, "Utilization of silica fume in concrete: Review of durability properties," *Resour Conserv Recycl*, vol. 57, pp. 30–35, 2011, doi: 10.1016/j.resconrec.2011.09.016.
- [56] U. Schneider, "Concrete at high temperatures - A general review," *Fire Saf J*, vol. 13, no. 1, pp. 55–68, 1988, doi: 10.1016/0379-7112(88)90033-1.
- [57] M. S. Bas and M. Y. Mansour, "The effect of cement dosage on mechanical properties of concrete exposed to high temperatures Ali Erg un," vol. 55, pp. 160–167, 2013.
- [58] A. A. Deshpande, D. Kumar, and R. Ranade, "Influence of high temperatures on the residual mechanical properties of a hybrid fiber-reinforced strain-hardening cementitious composite," *Constr Build Mater*, vol. 208, pp. 283–295, 2019, doi: 10.1016/j.conbuildmat.2019.02.129.
- [59] N. Yüzer, F. Aköz, and L. D. Öztürk, "Compressive strength-color change relation in mortars at high temperature," *Cem Concr Res*, vol. 34, no. 10, pp. 1803–1807, 2004, doi: 10.1016/j.cemconres.2004.01.015.
- [60] Q. Zhou and F. P. Glasser, "Thermal stability and decomposition mechanisms of ettringite at < 120 ° C," vol. 31, no. September 2000, pp. 1333–1339, 2001.
- [61] Q. Ma, R. Guo, Z. Zhao, Z. Lin, and K. He, "Mechanical properties of concrete at high temperature-A review," *Constr Build Mater*, vol. 93, pp. 371–383, 2015, doi: 10.1016/j.conbuildmat.2015.05.131.
- [62] W. Khaliq and F. Waheed, "Mechanical response and spalling sensitivity of air entrained high-strength concrete at elevated temperatures," vol. 150, pp. 747–757, 2017.
- [63] A. H. Akca, "High performance concrete under elevated temperatures," vol. 44, pp. 317–328, 2013, doi: 10.1016/j.conbuildmat.2013.03.005.
- [64] A. Behnood and H. Ziari, "Effects of silica fume addition and water to cement ratio on the properties of high-strength concrete after exposure to high temperatures," *Cem Concr Compos*, vol. 30, no. 2, pp. 106–112, 2008, doi: 10.1016/j.cemconcomp.2007.06.003.
- [65] U. Larisa, L. Solbon, and B. Sergei, "Fiber-reinforced Concrete with Mineral Fibers and Nanosilica," *Procedia Eng*, vol. 195, no. 3012, pp. 147–154, 2017, doi: 10.1016/j.proeng.2017.04.537.
- [66] P. S. Song and S. Hwang, "Mechanical properties of high-strength steel fiber-reinforced concrete," vol. 18, pp. 669–673, 2004, doi: 10.1016/j.conbuildmat.2004.04.027.
- [67] V. Tabak, "Effect of aspect ratio and volume fraction of steel fiber on the mechanical properties of SFRC," vol. 21, pp. 1250–1253, 2007, doi: 10.1016/j.conbuildmat.2006.05.025.
- [68] D. Gao, L. Zhang, M. Nokken, and J. Zhao, "Mixture Proportion Design Method of Steel Fiber Reinforced Recycled Coarse Aggregate Concrete," no. 100, pp. 1–16, 2019, doi: 10.3390/ma12030375.

- [69] F. Liu, W. Ding, and Y. Qiao, "Experimental investigation on the flexural behavior of hybrid steel-PVA fiber reinforced concrete containing fly ash and slag powder," vol. 228, 2019.
- [70] W. Alnahhal and O. Aljidda, "Flexural behavior of basalt fiber reinforced concrete beams with recycled concrete coarse aggregates," vol. 169, pp. 165–178, 2018.
- [71] H. Katkhuda and N. Shatarat, "Improving the mechanical properties of recycled concrete aggregate using chopped basalt fibers and acid treatment," vol. 140, pp. 328–335, 2017.
- [72] C. R. Gruz, "Elastic properties of concrete at high temperature," *Journal of the PCA Research and Development Laboratories*, vol. 8, no. 1, pp. 37–45, 1966.
- [73] V. Kodur, "Properties of Concrete at Elevated Temperatures," vol. 2014, 2014.
- [74] P. Pliya, A. Beaucour, and A. Noumowé, "Contribution of cocktail of polypropylene and steel fibres in improving the behaviour of high strength concrete subjected to high temperature," vol. 25, pp. 1926–1934, 2011, doi: 10.1016/j.conbuildmat.2010.11.064.
- [75] C. S. Poon, Z. H. Shui, and L. Lam, "Compressive behavior of fiber reinforced high-performance concrete subjected to elevated temperatures," vol. 34, pp. 2215–2222, 2004, doi: 10.1016/j.cemconres.2004.02.011.
- [76] N. Yermak, P. Pliya, A. Beaucour, A. Simon, and A. Noumowé, "Influence of steel and / or polypropylene fibres on the behaviour of concrete at high temperature : Spalling , transfer and mechanical properties," vol. 132, pp. 240–250, 2017.
- [77] W. Zheng, H. Li, and Y. Wang, "Compressive stress – strain relationship of steel fiber-reinforced reactive powder concrete after exposure to elevated temperatures," vol. 35, pp. 931–940, 2012.
- [78] G. Pachideh and M. Gholhaki, *An experimental study on the effects of adding steel and polypropylene fibers to concrete on its resistance after different temperatures*. ASTM International, 2019.
- [79] A. ASTM, "C150/C150M-17, standard specification for Portland cement," *Am. Soc. Test. Mater. West Conshohocken, PA, USA*, 2017.
- [80] C. Ag-, A. Machine, and M. Units, "Standard Specification for," 2013, doi: 10.1520/C0033.
- [81] S. Specification, "Standard Specification for Chemical Admixtures for Concrete 1," 2020, doi: 10.1520/C0494.
- [82] American Society for Testing & Materials, "C1240 - 14 Standard Specification for Silica Fume Used in Cementitious Mixtures," *Annual Book of ASTM Standards*, vol. i, pp. 1–7, 2012, doi: 10.1520/C1240-20.2.
- [83] ASTM C39, "Standard Test Method for Compressive Strength of Cylindrical Concrete Specimens 1," *ASTM Standard Book*, vol. i, no. March, pp. 1–5, 2003, doi: 10.1520/C0039.
- [84] C. C. Test, T. Drilled, and C. Concrete, "Standard Test Method for Flexural Strength of Concrete ( Using Simple Beam with Third-Point Loading ) 1," *Hand The*, vol. C78-02, no. C, pp. 1–4, 2010, doi: 10.1520/C0293.

- [85] G. Concrete, "Standard Practice for Capping Cylindrical Concrete Specimens 1", doi: 10.1520/C0617.
- [86] M. X. Xiong and J. Y. R. Liew, "Mechanical behaviour of ultra-high strength concrete at elevated temperatures and fire resistance of ultra-high strength concrete filled steel tubes," *Mater Des*, vol. 104, pp. 414–427, 2016, doi: 10.1016/j.matdes.2016.05.050.
- [87] "79 High-Strength Concrete at High Temperature – An overview.pdf."
- [88] C. C. Test, T. Drilled, C. Elements, U. Drilled, C. Cores, and C. Concrete, "Standard Test Method for Static Modulus of Elasticity and Poisson ' s Ratio of Concrete," vol. i, pp. 2–6, 2006, doi: 10.1520/C0469.
- [89] M. J. Heap *et al.*, "The influence of thermal-stressing ( up to 1000 ° C ) on the physical , mechanical , and chemical properties of siliceous-aggregate , high-strength concrete," *Constr Build Mater*, vol. 42, pp. 248–265, 2013, doi: 10.1016/j.conbuildmat.2013.01.020.
- [90] "Reproduced with permission of the copyright owner. Further reproduction prohibited without permission."
- [91] J. Bošnjak and A. Sharma, "Mechanical Properties of Concrete with Steel and Polypropylene Fibres at Elevated Temperatures," 2019, doi: 10.3390/fib7020009.
- [92] Z. P. Bažant, M. F. Kaplan, and Z. P. Bazant, "Concrete at high temperatures: material properties and mathematical models," 1996.
- [93] D. J. Pickel, J. S. West, and A. Alaskar, "Use of Basalt Fibers in Fiber-Reinforced Concrete.," *ACI Mater J*, vol. 115, no. 6, 2018.
- [94] H. Mohammad hosseini *et al.*, "Creep and drying shrinkage performance of concrete composite comprising waste polypropylene carpet fibres and palm oil fuel ash," *Journal of Building Engineering*, vol. 30, no. July 2019, p. 101250, 2020, doi: 10.1016/j.job.2020.101250.
- [95] H. Yang, L. Lv, Z. Deng, and W. Lan, "Residual compressive stress-strain relation of recycled aggregate concrete after exposure to high temperatures," no. September 2016, pp. 479–486, 2017, doi: 10.1002/suco.201500153.
- [96] H. Mohammad hosseini, F. Alrshoudi, and M. Tahir, "Journal of Building Engineering Durability and thermal properties of prepacked aggregate concrete reinforced with waste polypropylene fibers," *Journal of Building Engineering*, vol. 32, no. August, p. 101723, 2020, doi: 10.1016/j.job.2020.101723.
- [97] B. Demirel, "Effect of elevated temperature on the mechanical properties of concrete produced with finely ground pumice and silica fume," vol. 45, pp. 385–391, 2010, doi: 10.1016/j.firesaf.2010.08.002.
- [98] W. Yonggui, L. Shuaipeng, P. Hughes, and F. Yuhui, "Mechanical properties and microstructure of basalt fibre and nano-silica reinforced recycled concrete after exposure to elevated temperatures," *Constr Build Mater*, vol. 247, p. 118561, 2020, doi: 10.1016/j.conbuildmat.2020.118561.

- [99] M. Khan, M. Cao, and M. Ali, "Cracking behaviour and constitutive modelling of hybrid fibre reinforced concrete," *Journal of Building Engineering*, vol. 30, no. October 2019, p. 101272, 2020, doi: 10.1016/j.jobe.2020.101272.
- [100] M. Khan, M. Cao, and M. Ali, "Effect of basalt fibers on mechanical properties of calcium carbonate whisker-steel fiber reinforced concrete," *Constr Build Mater*, vol. 192, pp. 742–753, 2018, doi: 10.1016/j.conbuildmat.2018.10.159.
- [101] X. Wang, J. He, A. S. Mosallam, C. Li, and H. Xin, "The Effects of Fiber Length and Volume on Material Properties and Crack Resistance of Basalt Fiber Reinforced Concrete (BFRC)," *Advances in Materials Science and Engineering*, vol. 2019, 2019, doi: 10.1155/2019/7520549.
- [102] X. Sun, Z. Gao, P. Cao, and C. Zhou, "Mechanical properties tests and multiscale numerical simulations for basalt fiber reinforced concrete," *Constr Build Mater*, vol. 202, pp. 58–72, 2019, doi: 10.1016/j.conbuildmat.2019.01.018.
- [103] S. C. Lee, J. H. Oh, and J. Y. Cho, "Compressive behavior of fiber-reinforced concrete with end-hooked steel fibers," *Materials*, vol. 8, no. 4, pp. 1442–1458, 2015, doi: 10.3390/ma8041442.
- [104] M. Husem, "The effects of high temperature on compressive and flexural strengths of ordinary and high-performance concrete," *Fire Saf J*, vol. 41, no. 2, pp. 155–163, 2006, doi: 10.1016/j.firesaf.2005.12.002.
- [105] M. Hamza *et al.*, "Mechanical behavior of high-strength concrete incorporating seashell powder at elevated temperatures," *Journal of Building Engineering*, vol. 50, no. January, p. 104226, 2022, doi: 10.1016/j.jobe.2022.104226.
- [106] M. Usman, S. Hassan, M. Umair, and A. Hanif, "Axial compressive behavior of confined steel fiber reinforced high strength concrete," *Constr Build Mater*, vol. 230, p. 117043, 2020, doi: 10.1016/j.conbuildmat.2019.117043.
- [107] M. C. Nataraja, "Stress  $\pm$  strain curves for steel-<sup>®</sup> ber reinforced concrete under compression," vol. 21, 1999.
- [108] S. Ahmad, M. Rasul, S. K. Adekunle, S. U. Al-dulaijan, M. Maslehuddin, and S. I. Ali, "Mechanical properties of steel fiber-reinforced UHPC mixtures exposed to elevated temperature: Effects of exposure duration and fiber content," *Composites Part B*, 2019, doi: 10.1016/j.compositesb.2018.12.083.
- [109] W. Li and J. Xu, "Mechanical properties of basalt fiber reinforced geopolymeric concrete under impact loading," vol. 505, pp. 178–186, 2009, doi: 10.1016/j.msea.2008.11.063.
- [110] E. U. Khan, R. A. Khushnood, and W. L. Baloch, "Spalling sensitivity and mechanical response of an ecofriendly sawdust high strength concrete at elevated temperatures," *Constr Build Mater*, vol. 258, p. 119656, 2020, doi: 10.1016/j.conbuildmat.2020.119656.
- [111] K. Nisar, M. S. Siddique, M. Rizwan, S. H. Farooq, M. Usman, and A. Hanif, "Effect of multiwalled carbon nanotubes on compressive behavior of concrete at elevated temperature for mass concreting," *European Journal of Environmental and Civil Engineering*, vol. 0, no. 0, pp. 1–24, 2023, doi: 10.1080/19648189.2023.2194957.

- [112] C. C. Test, T. Drilled, C. Concrete, and S. T. Panels, "Standard Test Method for Flexural Performance of Fiber-Reinforced Concrete ( Using Beam With Third-Point Loading ) 1," pp. 1–9, 2009.
- [113] W. Khaliq and H. A. Khan, "High temperature material properties of calcium aluminate cement concrete," *Constr Build Mater*, vol. 94, pp. 475–487, 2015, doi: 10.1016/j.conbuildmat.2015.07.023.
- [114] V. R. Kodur, "Effect of Temperature on Thermal Properties of High-Strength Concrete NRC Publications Archive ( NPARC ) Archives des publications du CNRC ( NPARC ) Effect of temperature on thermal properties of high-strength concrete Web page / page Web," vol. 1561, no. April, 2003, doi: 10.1061/(ASCE)0899-1561(2003)15.